



LGS Wavefront Sensor Preliminary Design

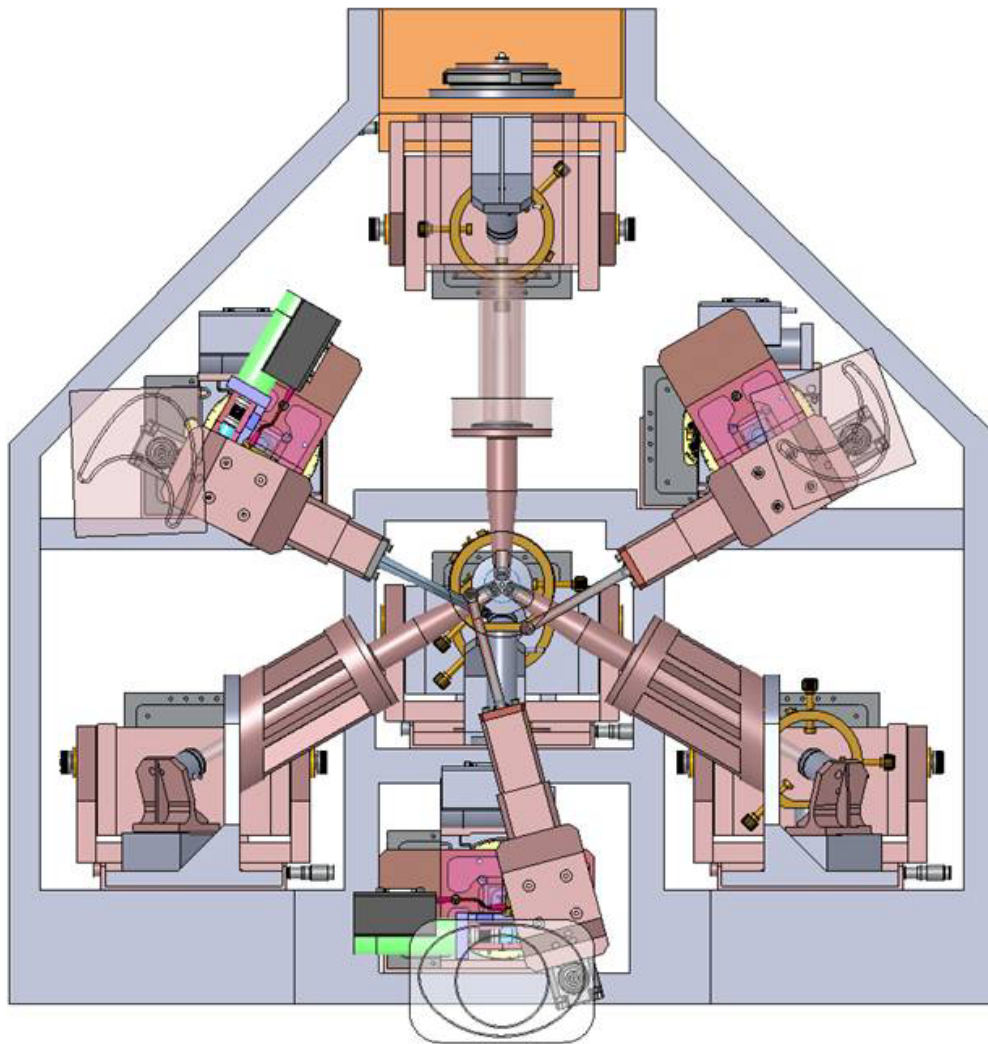
KECK ADAPTIVE OPTICS NOTE 692

Version 1.1

March 4, 2010

Viswa Velur, Alex Delacroix, and Richard Dekany

Caltech Optical Observatories





Revision History	
Version	Comments
0.9	First draft by Velur
1.0	Draft updated with input from Dekany and Delacroix
1.5	Updated document to address questions and commentary prior to mini-review
1.6	Document updated with clarifications and requirements compliance tables after Velur-Gavel-Kupke meeting at Lick Observatory



1 Introduction

1.1 Scope

This document describes the preliminary design of the Laser Guide Star Wavefront Sensors (LGS WFS) for Keck's Next Generation Adaptive Optics (NGAO) system. Version 1 of this document concentrates on key sensor design choices, the optical and mechanical preliminary design, and initial matters pertaining to calibration. It does not cover LGS WFS detector technology, camera operation, reliability, interfaces, or prototyping.

1.2 Architecture changes since the System Design Review

The LGS WFS subsystem design for NGAO has evolved considerably from the design presented at the NGAO System Design Review (SDR), driven primarily with the requirements and architecture changes flowing from Build-to-Cost (B2C) exercise ([KAON 642](#)). Most importantly, the original 5" – 50" radially scalable quincunx LGS asterism was set aside in favor of (Figure 1) the combination of a fixed LGS asterism, consisting of one LGS on-axis and three other LGS equally spaced at 10" radius, and a reconfigurable, or patrolling, LGS asterism whose purpose is not to provide high-order tomographic information, but rather to improve the science direction tip-tilt error indirectly, via *sharpening* of the NGS providing the science path tip-tilt measurement. The field of view (FoV) of the three Patrolling Asterism LGS WFS was also reduced during B2C from 150" to 120" diameter, corresponding to a similar reduction in LO WFS NGS field of regard (FoR).

To further simplify the architecture and ease implementation, the wavefront measurements from the Patrolling Asterism LGS WFS were also explicitly removed from the science-direction tomography solution and will be used exclusively to run three separate AO systems that sharpen the LO WFS NGS via a modified Multi-Object Adaptive Optics (MOAO) control strategy. (Further details on the Patrolling Asterism AO systems will be described in an upcoming KAON.)

Another significant post-SDR change is architectural decision to implement the LGS-stabilizing tip-tilt (TT) loop internal to the LGS WFS themselves, and not via an uplink TT mirror as is done for the current Keck AO systems. This approach provides for better control bandwidth as the time-delay between a measurement and TT correction is reduced by the round-trip propagation time of light traveling up and down to the Earth's mesospheric sodium layer.

Finally, the concept of a point spread function (PSF) monitoring camera in the Low Order Wavefront sensor (LO WFS) was abandoned for B2C, which implicitly transferred additional



importance for linear and stable LGS WFS calibration for purposes of telemetric AO PSF post-processing.

1.3 Reference documents

[KAON 551 Wavefront Sensor System Conceptual Design Report](#)
[KAON 511 - System Design Manual v2.1 \(doc\)](#), dated March 30th, 2008
[Preliminary Design Manual](#) (as of November 12th, 2009)
[KAON 685 - Opto-mechanical Design Document](#)
[KAON 666 - Fixed Pupil Mode](#)
[Flowdown Error Budget](#)
[KAON 642 - Design Changes in Support of Build-to-Cost](#)
[KAON 562 - LOWFS and LGS OSM conceptual study report DRAFT v3 \(doc\) \(pdf\)](#)

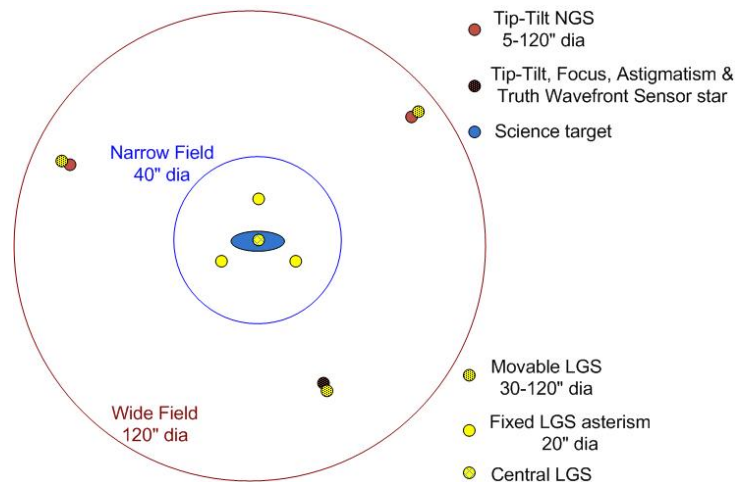


Figure 1- The Fixed LGS asterism consists of a 10" radius "3+1" configuration on-axis providing tomographic information for an on-axis science target, and three Patrolling LGS providing high-order wavefront information for image sharpening of the LO WFS NGS.

2 LGS WFS architecture

The basic functional relationships between the LGS WFS subsystem and other subsystems within the NGAO system are presented in Figure 2.

The basic function of the LGS WFS is to make wavefront phase measurements of the aberrations seen by the set of seven 589 nm LGS as it propagates downward back to Earth. The LGS WFS sends this data to the NGAO real-time-control (RTC) subsystem. The RTC uses the fixed asterism data to drive the low-order deformable mirror (LODM) and the high-order deformable mirror (HODM). Each patrolling LGS WFS data is used to drive the 32x32 actuator MEMS DM



in the corresponding LOWFS channel. The tip-tilt information from each of the 7 LGS WFS is used to drive the corresponding fast TT mirror in the LGS WFS itself. The AO control computer controls the position of the Patrolling Asterism LGS WFS in order to acquire return light from these movable LGS. It also provides configuration commands to the LGS WFS camera controllers, such as bias levels, gains, and frame rates. The LGS WFS camera controllers will provide in return status signals to the supervisory computer as a status monitor.

A more detailed schematic of the LGS WFS assembly is shown in Figure 3, divided into the three unique types of LGS WFS, namely a Patrolling WFS, an on-axis Fixed WFS, and a 10" radius Fixed WFS.

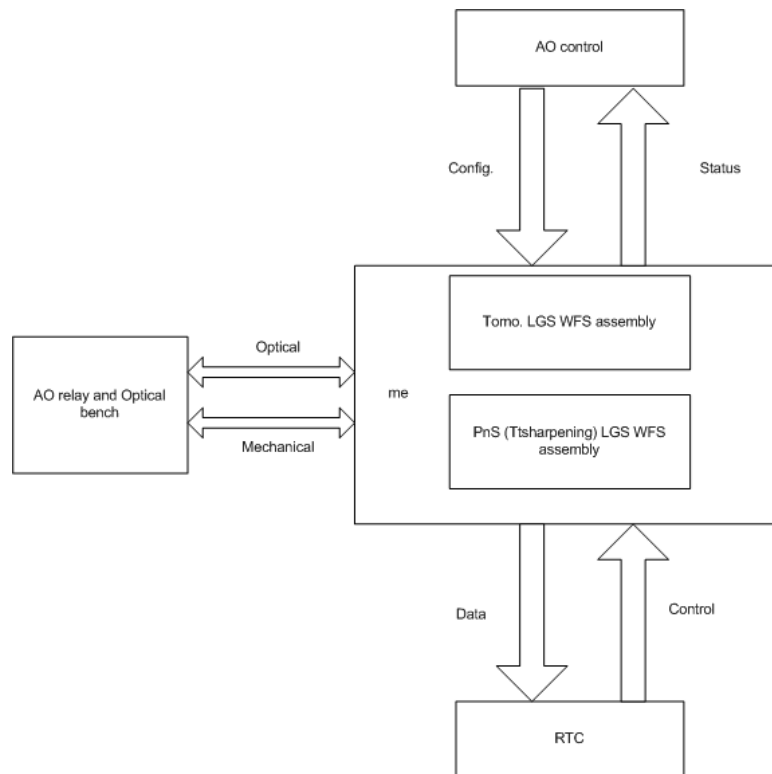


Figure 2- Context diagram of the LGS WFS showing the basic mechanical, optical and control interfaces to the AO system

The Patrolling WFS consists of a deployable theta-phi pick-off mechanism which includes the fast TT stabilization mirror, followed by an optical relay that provides slow pupil registration control as a function of patrol position in the field, followed by a Shack-Hartmann WFS. There is no need for any pupil derotation mechanism (erroneously suggested in KAON 562 and repeated in KAON 551).



The theta-phi Object Selection Mechanism (OSM) is preferred over an “R-phi” approach for NGAO LGS WFS because the naturally stable optical path length to the WFS is expected to reduce non-common-path (NCP) wavefront errors, and for commonality with the LO WFS OSM.

The two flavors of Fixed Asterism LGS WFS differ only in the detailed ordering of components in the optical train, driven by packaging constraints on the on-axis LGS WFS. These sensors utilize a set of three fixed, but otherwise identical to the Patrolling LGS, pick-off assemblies for the off-axis Fixed Asterism WFS, but not for the on-axis Fixed Asterism WFS.

The corresponding Zemax raytrace layouts of a Fixed Asterism LGS WFS and a Patrolling LGS WFS are shown in Figure 4 and Figure 5 respectively.

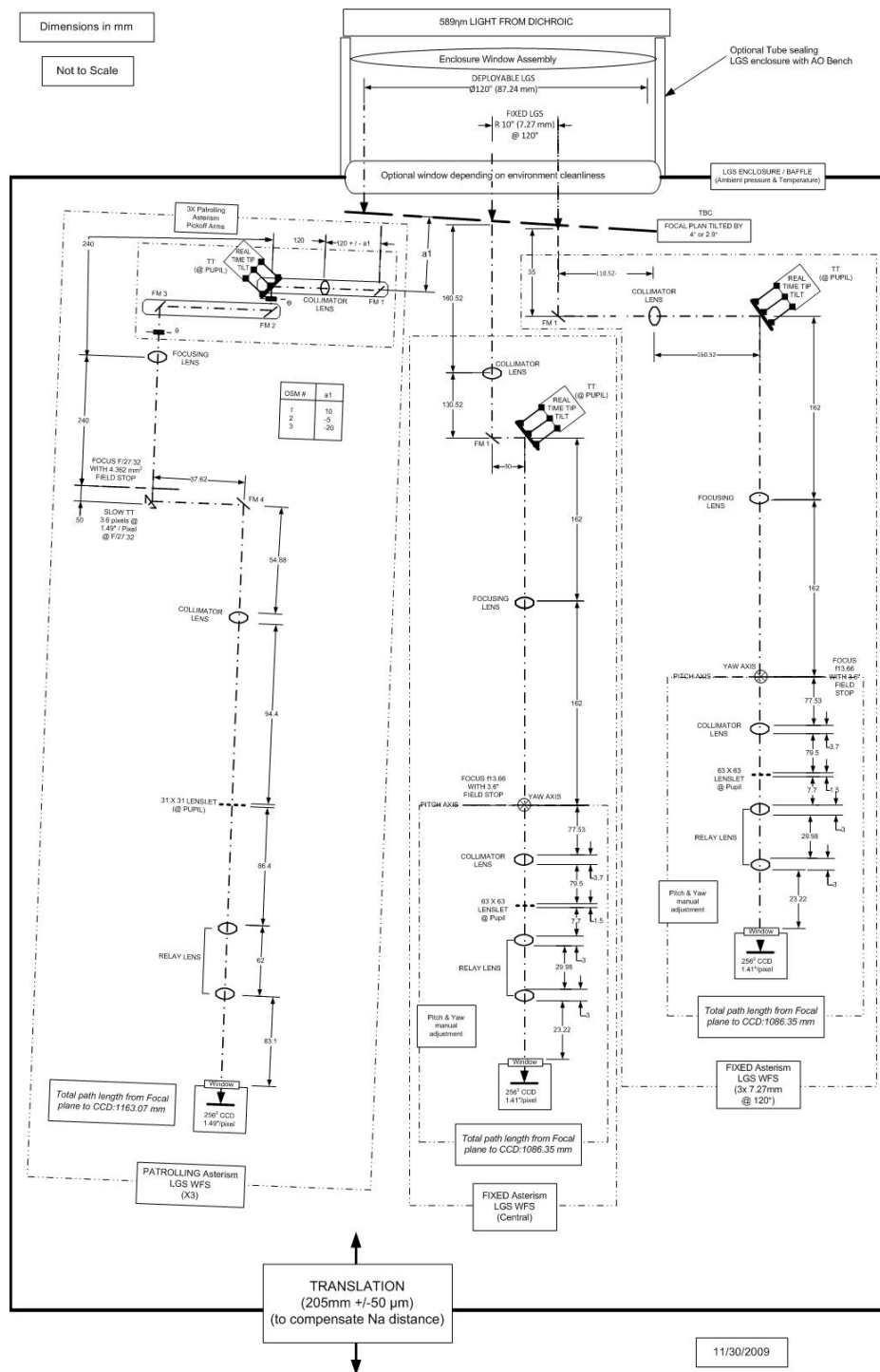


Figure 3 - Schematic of the LGS WFS assembly showing detail of one Patrolling WFS channel, the fixed central WFS channel and one fixed 10" radius channel.

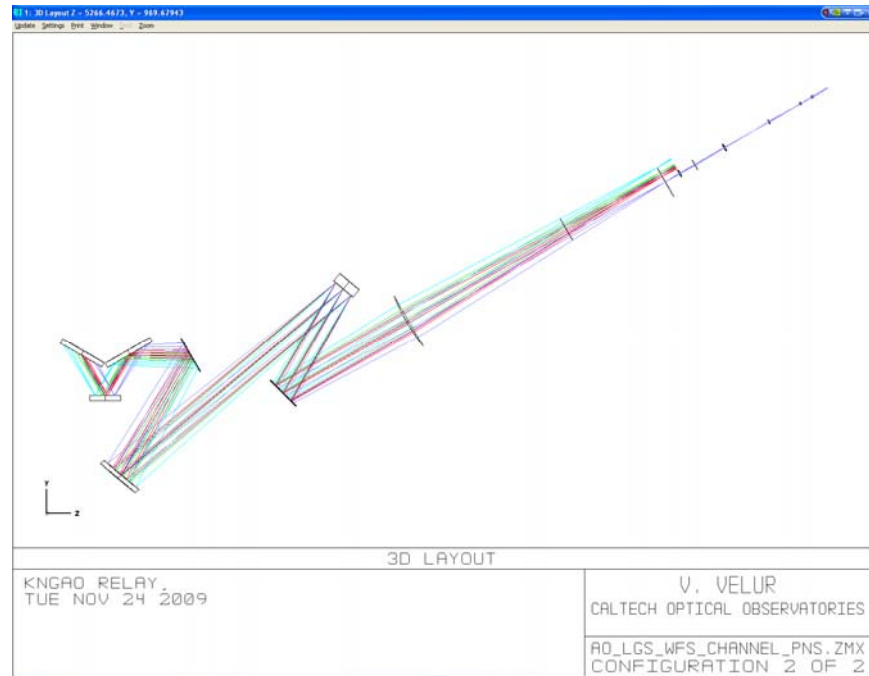


Figure 4 - Zemax layout of the entire optical train to a 10" radius Fixed Asterism LGS WFS CCD focal plane.

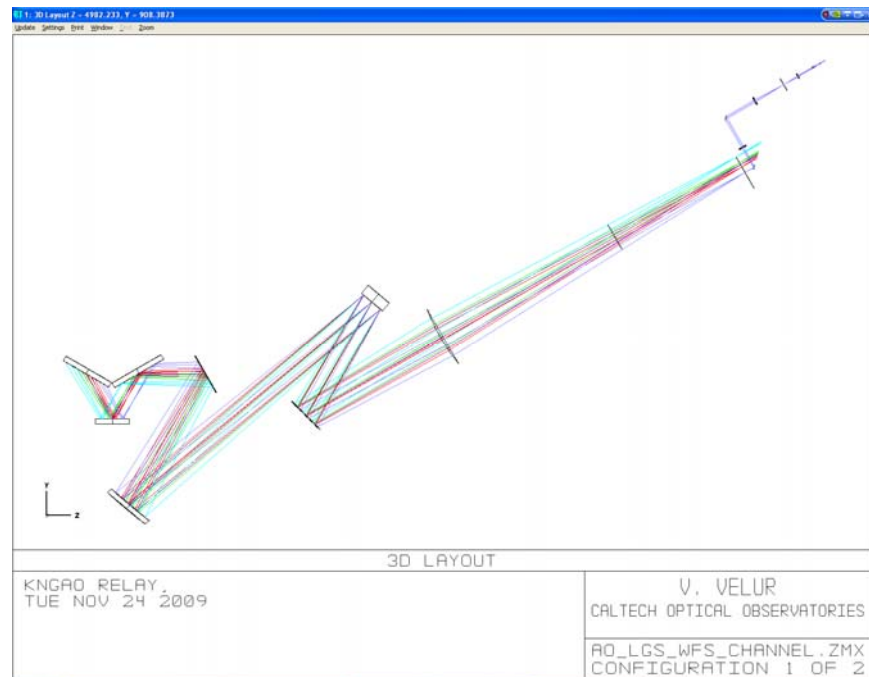
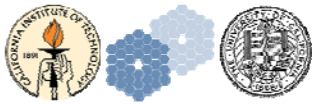


Figure 5 Zemax layout of the entire optical train to a Patrolling Asterism LGS WFS CCD focal plane (shown at full 60" field radius).



3 LGS WFS Support Structure

As shown in Figure 6, the LGS WFS does not enjoy the structural support of the AO relay optical bench in the current design concept, and so must provide its own stable structural support, mounting interface to the Nasmyth platform, and thermal stability with respect to optical components within the cold enclosure on the AO relay optical bench. *[Note: Detailed consideration of the LGS WFS structure will occur later in the PD phase.]*

4 LGS WFS fore-optics

The LGS light path through the NGAO wide-field relay is shown in Figure 7. Sodium light from the telescope traverses through the entrance window (not shown), the K mirror and the fold followed by the 1st off-axis-paraboloid (OAP), after which it is incident on the LODM. Following the LODM it is folded out of collimated space by a notch dichroic onto (nominally) a 1-m focal length plano-convex lens that focuses the beam. *[Note: This lens assembly may evolve during the remainder of the PD phase and should be more generally considered a window assembly, because although it is currently considered part of the LGS WFS subsystem, it provides a key thermal and humidity seal for the AO wide-relay cold enclosure.]*

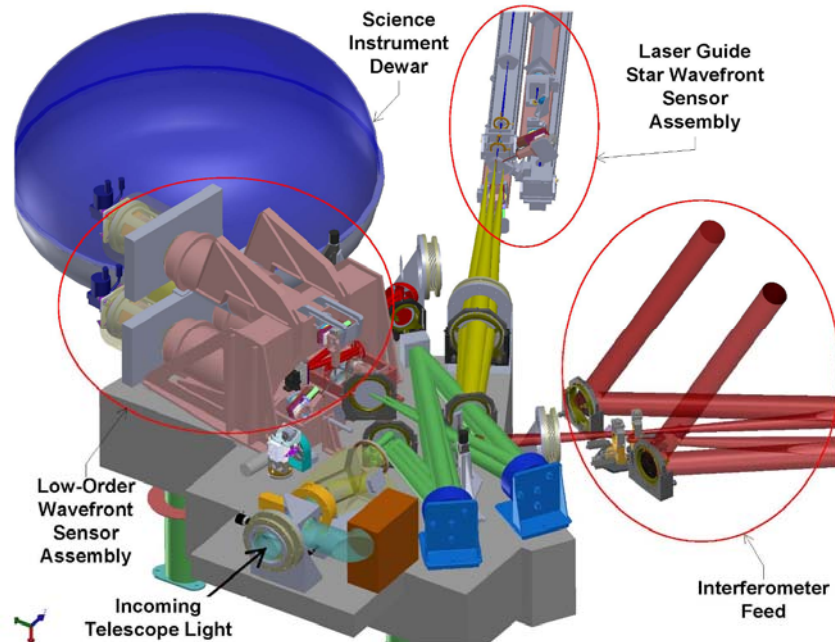


Figure 6 - NGAO optical layout showing the location of the LGS WFS assembly with respect to the rest of the system (courtesy C. Lockwood, UCO Lick). *(Note: This image does not contain the PD phase LGS WFS solid model.)*



4.1 Input Optical Aberrations

Laser light, passing through the wide-field relay at conjugate distances markedly different than the design-optimized infinite distance for science light, suffers considerable optical aberration. Figure 8 shows the optical spot diagrams for LGS beams delivered by the AO relay originating at a Na layer distance of 90 km. The Fixed LGS spots delivered by the AO relay have RMS radii between 26 and 45 μm at the LGS pick-off plane, while the Patrolling LGS spots sizes range between 130 and 150 μm RMS radius.

As the working F/# at the LGS pick-off is 13.56 at 22 degrees off zenith, one arcsecond of angle on-sky corresponds to 720 μm at the LGS focal plane (based on Version 7 of the NGAO optical design), indicating contributions to sensor subaperture PSF FWHM (which are 2.355 times larger than the spot diagram RMS radius) as follows:

	On-sky field point	Full-beam RMS spot size radii (from Zemax)	Corresponding Full-beam FWHM	LGS WFS Subaperture RMS spot size radii (from Zemax)	Corresponding LGS WFS Subaperture FWHM
Fixed Laser Asterism WFS	10 arcsec	26 to 45 μm	83 to 147 mas	negligible	negligible
Patrolling Laser Asterism WFS	60 arcsec	130 to 150 μm	425 to 491 mas	< 6 μm	< 20 mas

Table 1. Contribution to image quality degradation at the LGS WFS input focal plane and at the back-end WFS subaperture focal plane.

Although the entire beam has large aberrations, the image quality functional requirement is that the optical relay and WFS combination not induce more than of 0.25" FWHM to image width *in the subaperture*. As was discussed in KAON 685 “NGAO Optical Relay Design”, the degradation in a subaperture is considerably less than over the entire beam, as much of the aberration in the beam leads to subaperture spot displacement and not image blurring within the subaperture. *[Note: A system-level allocation of the allowable optical error contributions is being made in parallel to the writing of this document.]*

As an independent check on the effect of large input aberrations, we evaluated the performance of a single subaperture 1/31st of the diameter of the primary mirror and de-centered this aperture using Zemax to look at the resulting impact on spot size. One can see RMS spot radius of almost 6 μm (corresponding to $6/720 \times 2.355 = 20$ mas FWHM) at the worst-case field angle as is shown by Figure 9 and Figure 10, and summarized in Table 1. This is a small compared to the 250 mas FWHM allocation to subaperture image quality degradation.

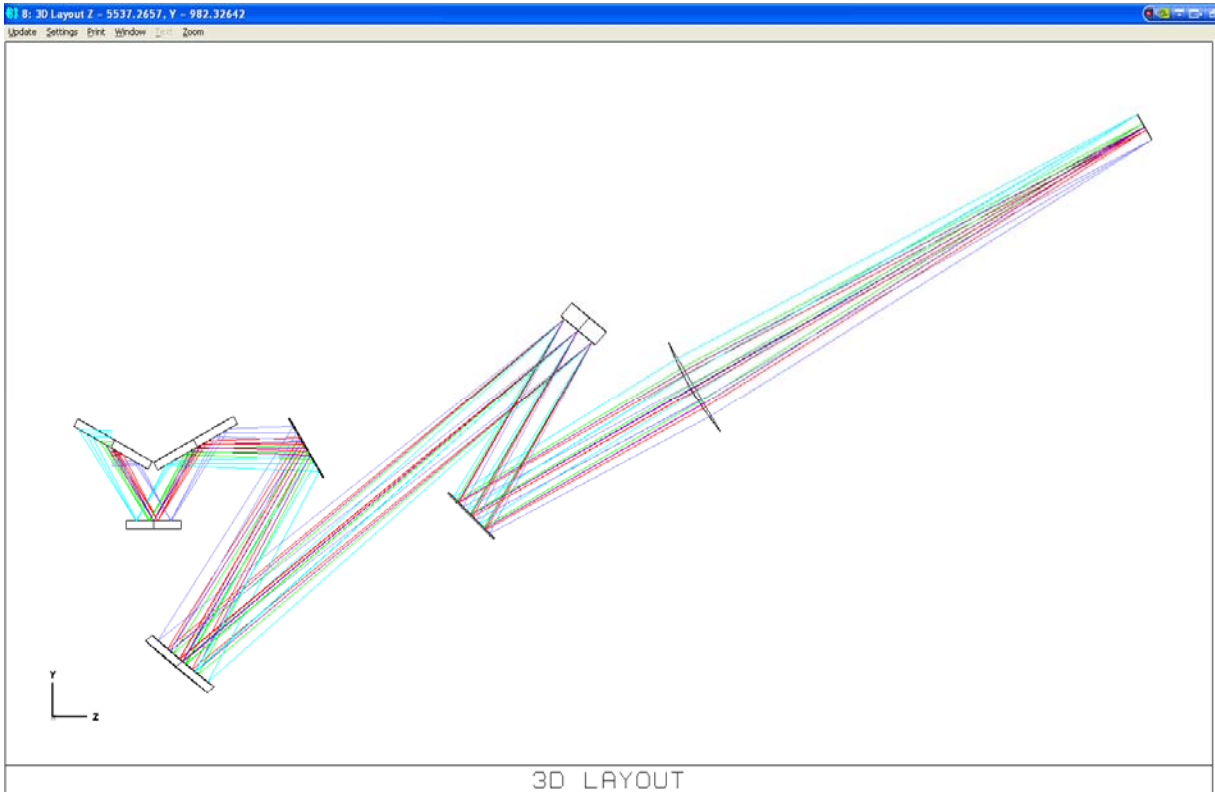


Figure 7 - Laser guide star light path starting from the K mirror to the LGSWFS pick-off focal plane.

It is useful to note that the LGS input focal plane delivered by the AO system is both curved and tilted. The curvature of the focal plane varies between 883 mm and 2604 mm as the distance to Na-layer varies from 90 to 180 km (we will commonly quote 90 km and 180 km distances, though the requirements for LGS distance vary between 81 and 282 km (TBC)).

In summary, the optical quality of the combination of the wide-field optical relay (as described in KAON 685, dated Nov 17, 2009) and the LGS WFS designs presented here meet the allocated degradation to image quality, in terms of design aberrations. A more detailed error budget flowdown that includes design, alignment, and fabrication tolerances, however, is still needed.

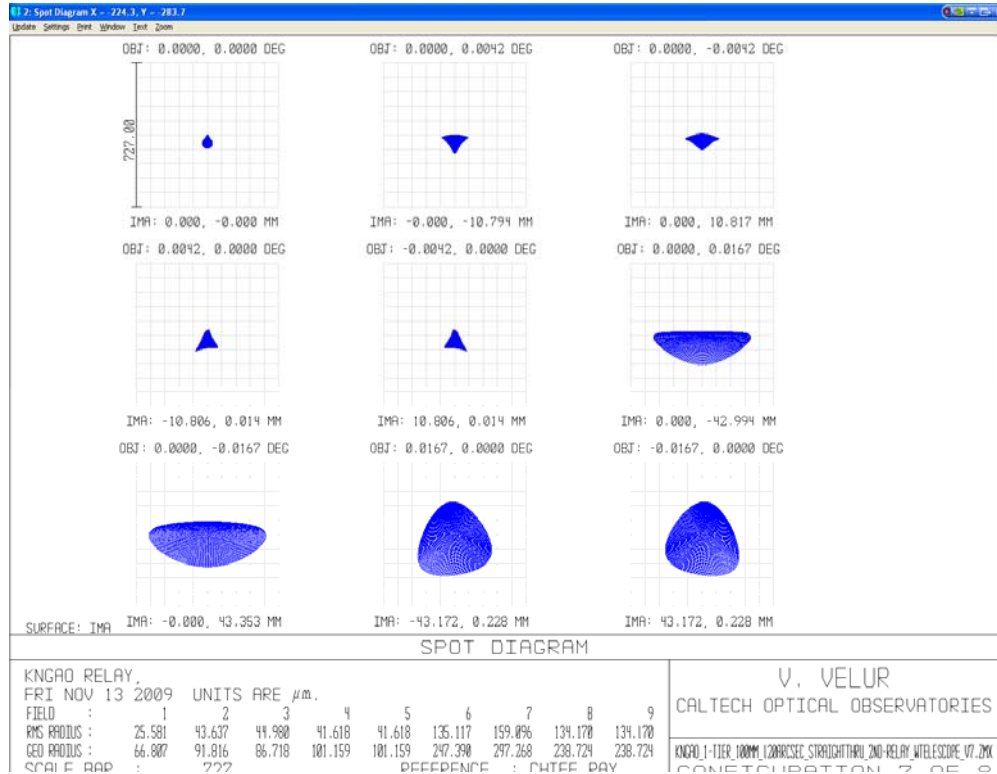


Figure 8 - LGS WFS spots when the telescope is pointing at zenith, indicating relatively large relay errors over the Patrolling WFS 120" FoR. The first spot is the on-axis spot diagram followed by spot diagrams at the X and Y extremities of the narrow science field. The last 4 points show the spots as seen at the X and Y extremities of the 120" diameter LGS FoR [For reference – 66.8 μm and 297 μm RMS spot sizes correspond to 91 and 409 mas .]

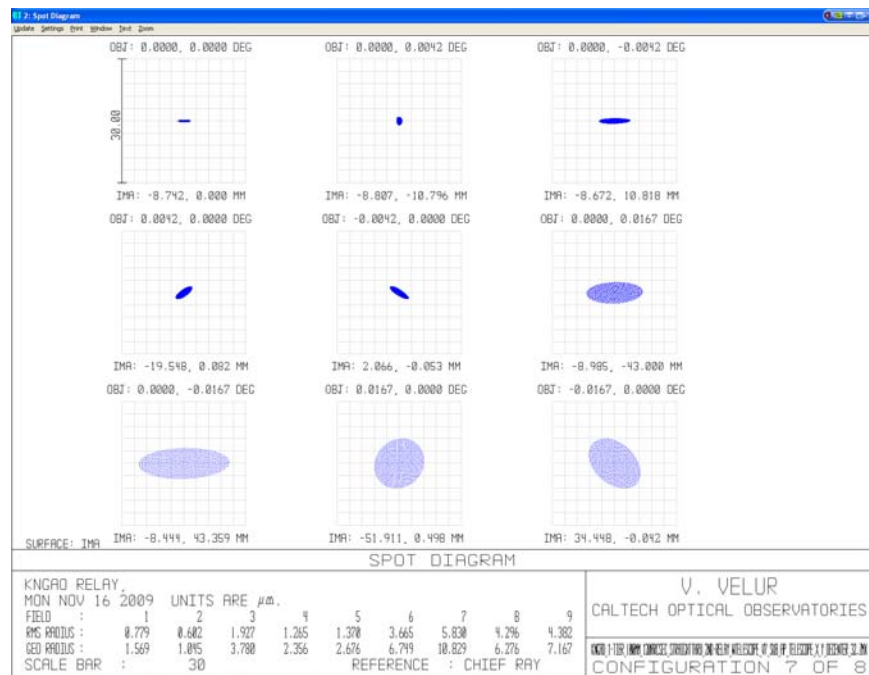




Figure 9 - LGS spots as seen by a single Patrolling LGS WFS sub-aperture. The spots diagram was generated by creating a de-centered aperture that is $1/31^{\text{st}}$ the size of the Keck primary mirror and making the entrance pupil the size of a single sub-aperture. The aperture parameter in the Surface Property Menu was set to the primary mirror radius (5297.9 mm) to accommodate ray tracing. The worst case sub-aperture spots see a 6 μm (RMS) radius. [For reference – 1.569 μm and 10.029 μm geometric spot sizes correspond to 2.14 and 14.8 mas.]

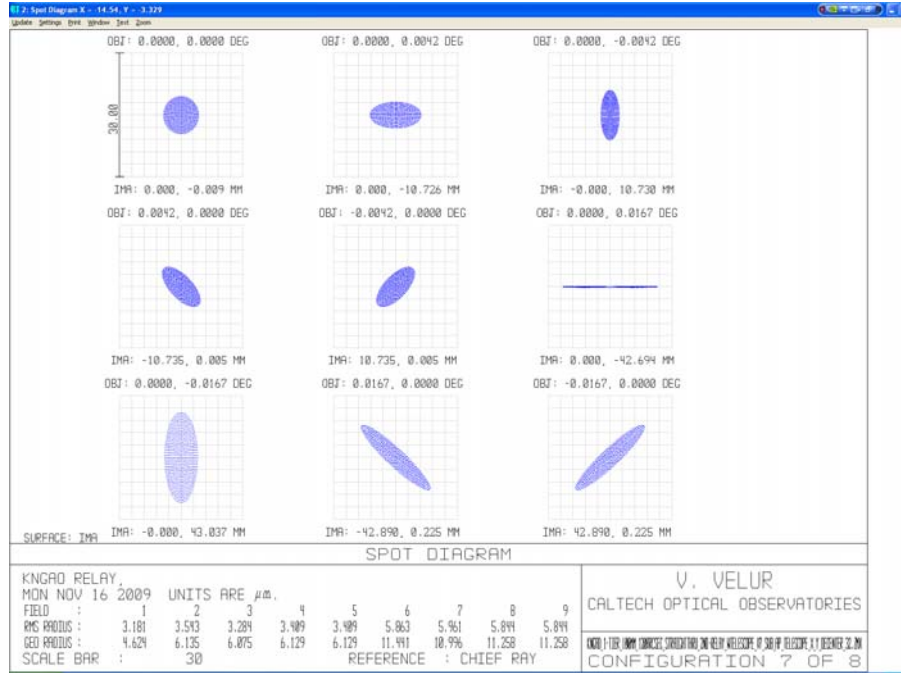


Figure 10 - LGS spots as seen by a Patrolling Asterism LGS WFS sub-aperture (de-centered in the orthogonal direction with respect to Figure 9). Worst case sub-apertures are 6 μm (RMS) radius. [Note that the fixed asterism spots have little aberration at the sub-aperture level.]

In conclusion, there is adequate leeway for a LGSWFS design within the error budget allocation for both the fixed and the patrolling LGSWFSs as the sub-aperture level aberrations are small compared to what the sub-aperture is capable of measuring. The worst case subaperture level spot shift due to aberration from the AO optical train in the fixed LGS WFSs is 15 mas and that in the Patrolling LGSWFS's is 15.5 mas.

5 Shack-Hartmann WFS Design

5.1 Relevant analysis for design

5.1.1 WFS Pixel Angular Scale

From experience we know that characterizing and calibrating each sub-aperture of the seven LGS WFS for non-linearity is non-trivial and hence we choose plate-scales to ensure that each sensor operates in its linear regime. Pixel scale is chosen based on the apparent spot size FWHM



expected to be realized within each of the WFS (sans charge diffusion). Figure 11, extracted from the WFE Budget v1.48, shows the apparent spot size for the tomographic WFS (left column) and WFS (right column). For the fixed LGS asterism, the 1-D tilt error is 50 mas and the diffraction limited sub-ap spot size is 699 mas (this corresponds to one wave of tilt in the sub-aperture). We choose $p = 0.5$ from Table 2 to accommodate capture range and linear operating regime. The central fixed LGS guide stars have little differential tilt and so the RMS 1D tilt of each beacon is small, with $p = 0.5$, the sub-aperture is capable of measuring ± 1.5 waves (or 1.05 arcsec) with negligible loss in linearity. $P < 0.5$ was considered to aggressive a design parameter and not considered. For the variable asterism the 1D tilt error is ~ 100 mas and the sub-aperture diffraction limited spot size is 343 mas (this corresponds to one wave of tilt in the sub-aperture). We choose $P=1.0$ for this sensor based on Table 2 to be able to measure ± 2.5 waves (± 0.86 arcsec) of tilt.

Based on work done by Thomas¹² the p-value selection seems reasonable. The LGSWFS sensor team will send the exact NGAO LGSWFS parameters to Ms. Thomas for verification of p-value selection.

Detector size per subaperture	Pixel Size/ spot size (p)	Useful tilt range +/- waves	Departure from linearity (waves)
2x2	1.0-1.5	0.5	0.024
2x2		1.0*	.13*
4x4	0.5	1.5	0.019
4x4	0.67	2	0.085
4x4	1	2.5	0.19

* - nonlinear response

Table 2 - Dynamic range and linearity of Shack-Hartmann quad-cells (this is same as Table 5.3, Pg. 149 of Hardy). NGAO Patrolling LGS WFS's use a 4x4 pixel sub-aperture with $p=1$; while we choose $p= 0.5$ for the Fixed LGS WFS's. [Note – 0.019 waves of non-linearity corresponds to 11 nm of systematic error in the WFS, 0.085 waves corresponds to 47 nm and is unacceptable for the (tomography) LGS WFS. The allocation for the systematic error due to non-linearity for the fixed LGS sensors is 20 nm(?)]



Fixed LGS spot size calc.

Laser Guide Star Size Calculation	
Finite Object Size	
Intrinsic guide star diameter	0.00 arcsec
Uplink formation of the beacon(s)	
Perfect Uplink AO?	NO
Inherent aberrations in the uplink beam:	0.90 arcsec
Beam movement contribution to uplink	0.27 arcsec
Residual seeing contribution to uplink	0.47 arcsec
Diameter of point source laser at Na layer:	1.02 arcsec
Seeing	
Natural seeing FWHM at GS wavelength	0.46 arcsec
Subaperture Tip/Tilt corrected FWHM	0.36 arcsec
AO-compensated FWHM	0.06 arcsec
Contribution due to seeing	0.36 arcsec
Elongation	
Distance from LLT to telescope axis:	0.00 m
Use Max. Elongation?	NO
Avg. Elongation	0.99 arcsec
Contribution to FWHM due to elongation	0.49 arcsec
System Aberrations	
Aberrations in AO thru to WFS	0.25 arcsec
Atmospheric Dispersion	
ADC in HOWFS?	NO
RMS blurring due to atmospheric dispersion	0.000 arcsec
Total size of detected return beam:	1.21 arcsec
Sensing Approach	
Pyramid WFS?	NO
Charge Diffusion	
Charge Diffusion	0 pixels
Contribution due to Charge Diffusion	0.00 arcsec
Subaperture Diffraction	
Lambda/d (for sensing)	0.71 arcsec
Spot size used for centroiding	
	1.41 arcsec

Patrolling LGS spot size calc.

Laser Guide Star Size Calculation	
Finite Object Size	
Intrinsic guide star diameter	0.00 arcsec
Uplink formation of the beacon(s)	
Perfect Uplink AO?	NO
Inherent aberrations in the uplink beam:	0.90 arcsec
Beam movement contribution to uplink	0.27 arcsec
Residual seeing contribution to uplink	0.47 arcsec
Diameter of point source laser at Na layer:	1.02 arcsec
Seeing	
Natural seeing FWHM at GS wavelength	0.46 arcsec
Subaperture Tip/Tilt corrected FWHM	0.39 arcsec
AO-compensated FWHM	0.06 arcsec
Contribution due to seeing	0.39 arcsec
Elongation	
Distance from LLT to telescope axis:	0.00 m
Use Max. Elongation?	NO
Avg. Elongation	0.93 arcsec
Contribution due to elongation	0.93 arcsec
System Aberrations	
Aberrations in AO thru to WFS	0.25 arcsec
Atmospheric Dispersion	
ADC in HOWFS?	NO
RMS blurring due to atmospheric dispersion	0.000 arcsec
Total size of detected return beam:	1.45 arcsec
Sensing Approach	
Pyramid WFS?	NO
Charge Diffusion	
Charge Diffusion	0.00 pixels
Contribution due to Charge Diffusion	0.00 arcsec
Subaperture Diffraction	
Lambda/d (for sensing)	0.36 arcsec
Spot size used for centroiding	
	1.49 arcsec

Figure 11 - Apparent spot size at the detector due to various effects for the fixed tomographic LGS WFS spots (left) and the apparent spot size at the detector of Patrolling WFS (TT sharpening) LGS WFS spots (right). Charge diffusion term is set to 0 here in order to make an optical estimate of FWHM, which is appropriate for determining the detector pixel scale. *[The EBS models charge diffusion and so will the final system when transfer curve calibration is performed on the as-built system.]*

5.1.2 Stabilization TT Mirror Specification

To determine the TT mirror of choice, we need to specify the resolution and the throw required for the mirror given the bandwidth requirement from the requirements database.

$$\text{Pupil de-magnification at the TT mirror} = 10.949 \text{ m} / (12.5 \text{ mm} / 1000 \text{ mm/m}) = 875.92$$



TT resolution on sky = 1 milliarcsec (say)

[The RMS 1D tilt error is 95 milliarcsec (c.f. EBS Version 1.48)]

Hence, TT mirror resolution = $0.001 \text{ (arcsec)} * 875.92 = 0.875 \text{ arcsec} = 42 \text{ microradians}$

Capture range required is 2 arcsec or $2 * 875.92 \text{ ''} / 206265 \text{ (''/rad)} = 8.49 \text{ millirad}$ (we can position the laser beacons with slow moving mirrors to 2 arcsec precision on sky)

Based on the resolution and the capture range we choose the following mirror from Physik Instrumente's catalog:

<http://www.physikinstrumente.com/en/products/prspecs.php?sortnr=300700>

S-330.8SL has 10 mrad of tilt travel with 0.5 microrad (0.12 milliarcsec resolution on sky) open-loop resolution is the mirror of choice. The mirror has a resonance frequency of 1 kHz with a 1" diameter optic with 1/4" thickness.

5.1.3 Evaluation of Differential Focus & Impact of Single LGS WFS Focus Stage

Individual LGS WFS channels see differential focus due to two effects; viz. change in radius of curvature (RoC) of the LGS focal plane with change in distance to the sodium layer (c.f.) and due to the finite size of the LGS asterism on sky. The physical distance between the innermost and outermost laser beacons on-sky vary with zenith angle as shown in ; this effect is quantified in . Both effects, though not negligible, are entirely deterministic given the position and geometry of the LGS asterism and so the defocus can be calibrated away by the RTC. So the preferred design choice is to use a single focusing stage for the entire LGS WFS assembly, while noting that *this requires additional requirement(s) on the RTC to apply this calibration as a changing function of zenith angle.*

Dist. To Na layer	ROC of focal plane (mm)	focal plane size (mm)	Sag (um)	Delta sag (um)	Error (in waves) after splitting the difference
PnS asterism					
90 km	883.20	87.24	1077.82		
180 km	2064.00	87.24	460.98	616.84	0.5236
Fixed LGS asterism					
90 km	883.20	7.27	7.48		
180 km	2064.00	7.27	3.20	4.28	0.0036

Table 3 - Radii of curvature of the LGS focal plane as delivered by the NGAO optical relay at 90 and 180 km Na layer object distance and the change in focus due to the changing RoC.

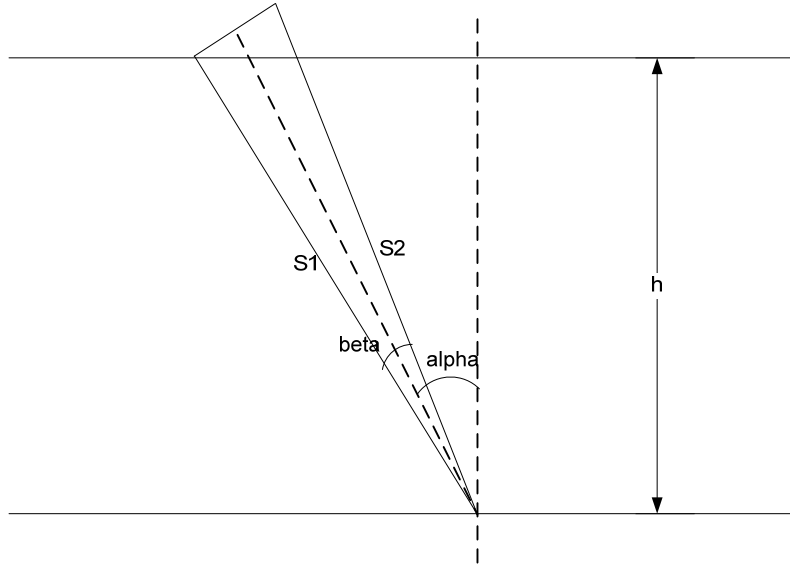


Figure 12 - Schematic showing defocus between the innermost and outermost LGS due variation in physical distance of those with zenith angle.

Figure 12 shows a simplistic representation of LGS beacons being created at the sodium layer from a central launch telescope:

$$\alpha = 1.22 \text{ radians (with the telescope pointing 70 degrees off-zenith pointing)}$$

$$\beta = 9.70\text{E-}05 \text{ to } 5.82\text{E-}04 \text{ radians (for 20-120 arcsec LGS asterism diameter)}$$

$$b = h / \cos(\alpha) * \beta$$

$$x = b * \tan(\alpha)$$

Where, α is the telescope zenith angle.

β is the angle subtended by the LGS asterism

h is the Na layer height at zenith (e.g. 90 km)

b is the physical diameter of the asterism (ignoring tilt anisoplanatism) at the Na layer

x is the object distance shift between the nearest and furthest LGS beacon.

$x/2$ is the object shift of an outermost LGS relative to the central LGS.



Guide star asterism diameter	Defocus error due to geometry of the asterism (um), x/2	Error in waves (220 um corresponds to $\lambda/4$ depth of focus)
10	6.5	0.006 waves
120	68	0.0773 waves

Table 4 - Error due to change in focus between the innermost and outermost LGS with zenith angle. For reference $\lambda/4$ depth of focus is 147 nm of WFE and 219 um of defocus (as given by $2*\lambda*F/\#2$). The difference between S1 and S2 in figure in is seen as a defocus at the LGS focal plane and this difference is evenly split between the innermost and outermost beacons.

5.1.4 LGS WFS Relay Optical Aberration Specification

Total aberration allocation for the NGAO relay and LGS WFS is, according to WFE Budget v1.48, a FWHM of 0.25". Internal WFS aberration allocation as part of this total error budget has not been allocated via the Flowdown process. For the remainder of this document, therefore, we will assume an allowable contribution from the LGS WFS itself of the entire 0.25" FWHM, and will revise this document as warranted.

The LGS spots delivered by the OSM are 3 and 8 times smaller in radii (RMS) than the input spots from the AO wide-field relay for the Fixed and Patrolling LGS WFS's respectively. The OSM's contribution corresponds to an FWHM of $\sim 0.05''$. Hence, the LGS WFS relay performance needs to have:

Geometric spot size (RMS as indicated by Zemax) at the detector =

Error budget allocation (in arcsec/ FWHM) / 2.355 (FWHM/RMS) * 21 (um/pixel) / 1.49 (arcsec/pixel) = $0.25 / 2.355 * 21 / 1.49 = \sim 1.5 \text{ um}$

Where we've assumed the plate scale from the Patrolling Asterism WFS (using the Fixed Asterism WFS plate scale (0.705 arcsec/pixel, the spec would be $\sim 3.2 \text{ um}$)

5.1.5 Field Stop Specification

The FoV of the Fixed and Patrolling WFS sub-apertures are 2.82 and 5.64 arcsecs respectively. A square- field stop that is 2.8 arcsec and 5.64 arcsec on edge will be positioned at the respectively at each of the fixed and Patrolling LGSWFS focus to prevent cross-talk of LGS spots at the detector. The potential advantage of this field stop to also serve as a wavefront anti-aliasing filter will also be explored during the PD phase.



5.2 Optical Design and Performance

5.2.1 Fixed LGS WFS

5.2.1.1 Fixed Asterism WFS Design Parameters

As indicated in Section 5.1.1, the p-value of the Fixed LGS WFS is 0.5, making the pixel size/spot size = 0.5. Hence, 1.41" on-sky corresponds to two detector pixel (42 μm). From the NGAO optical design, we know that 720 μm at the LGS focal plane corresponds to 1" on-sky.

Plate Scale Ratio (PSR) = $f_{\text{collimator}}/f_{\text{lenslet}} * 1/m =$

$$\text{Input plate (um/asec)} / \text{Detector plate scale (um/asec)} = 720/29.78 = 24.4064,$$

where, m is the de-magnification between the lenslet spots and the detector.

We choose a commercial collimator (JML Optical's 80 mm best-form lens) instead of a commercial lenslet as the Fresnel Number (FN) of the lenslet is an invariant in the design and any commercial lenslet needs to have the exact required FN to be used in NGAO. The limited lenslet database we have didn't have any match for the required lenslet FN. In the future, we intend to look at the cost savings vs. performance impact of selecting a non-optimal, but commercially off-the-shelf lenslet array.

The pitch of the lenslet array is given by, $d_{\text{each lenslet}} = f_{\text{collimator}}/f\# * 1/(\# \text{ of sub-aps}) = 80/13.56 * (1/63) = 93.6 \mu\text{m}$

The de-magnification, $m = 0.084/0.0936 = 0.896$

The focal-length of the lenslet is, $f_{\text{lenslet}} = f_{\text{collimator}}/m * (29.78/720) = 3.68 \text{ mm}$. The f/# of the lenslet = 39.42.

The Fresnel # (FN#) of the lenslet array is $\text{FN\#}_{\text{lenslet}} = (d_{\text{each lenslet}}/2)^2/(f*\lambda) = 1.01$.

The $\text{FN\#}_{\text{lenslet}}$ term is an invariant in the design given plate-scales, the number of subapertures, and centroiding geometry. It can also be expressed as $1/(4*\lambda) * (D_{\text{telescope}}/\# \text{ of subaps}) * (\text{spot sep. in radians})$.

5.2.1.2 Fixed Asterism Pick-off Relay

To accommodate mechanical packaging constraints and provide an internal stabilization tip-tilt mirror pupil location, while keeping the optical surfaces to a minimum, a 1:1 relay was chosen to transfer the native output focal plane from the NGAO wide-angle relay to an intermediate internal focus position within the LGS WFS. Figure 13 and Figure 14 show the optical layout of the relay (total optical length 640 mm) and spot diagrams they deliver. The pick-off relay has a FoV of 5" and is designed to be telecentric in order to not introduce any spurious tilts in the beam due to the incidence position of the LGS light on the pickoff. The spots sizes are 16 μm



RMS compared to 40 μm RMS spots that the AO relay generated. The design for the pick-off is available at:

http://www.oir.caltech.edu/twiki_oir/pub/Keck/NGAO/WFS/fixed_LGS_pick_off.ZMX

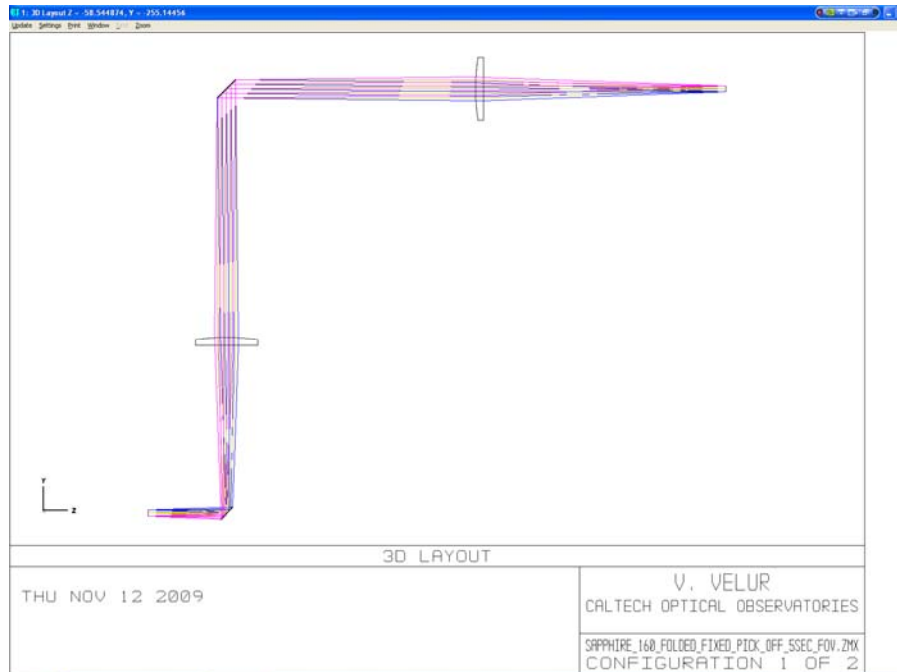


Figure 13 - Telecentric 1:1 Fixed LGS WFS pick off relay. The total length of the relay is 640 mm (limited by packaging constraints).

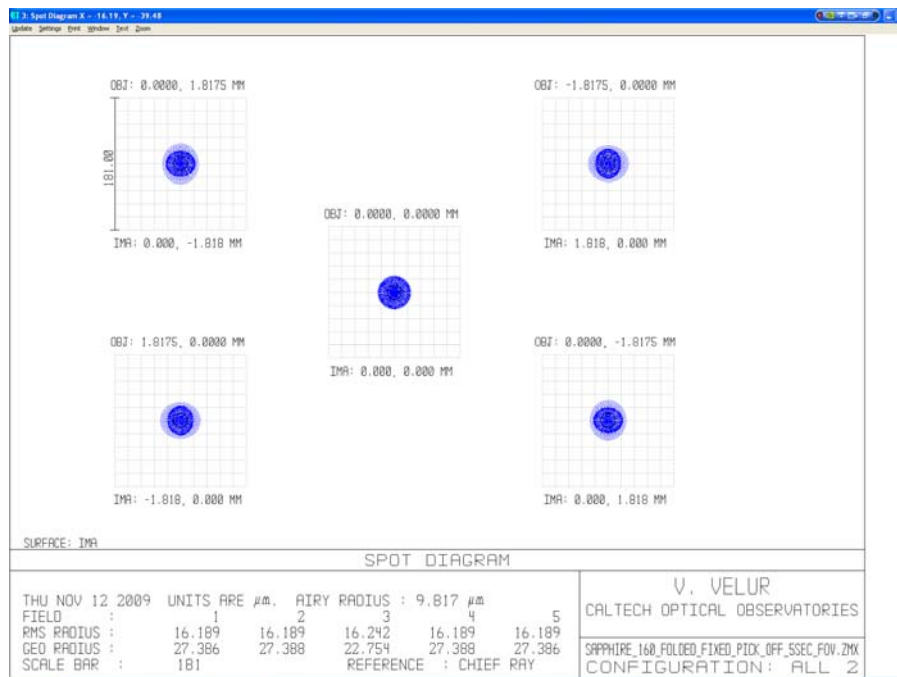




Figure 14 - Spot diagram showing the performance of the fixed LGSWFS pick-off over a 5 arcsec FoV (scale bar corresponds to $\frac{1}{4}$ arcsec.).

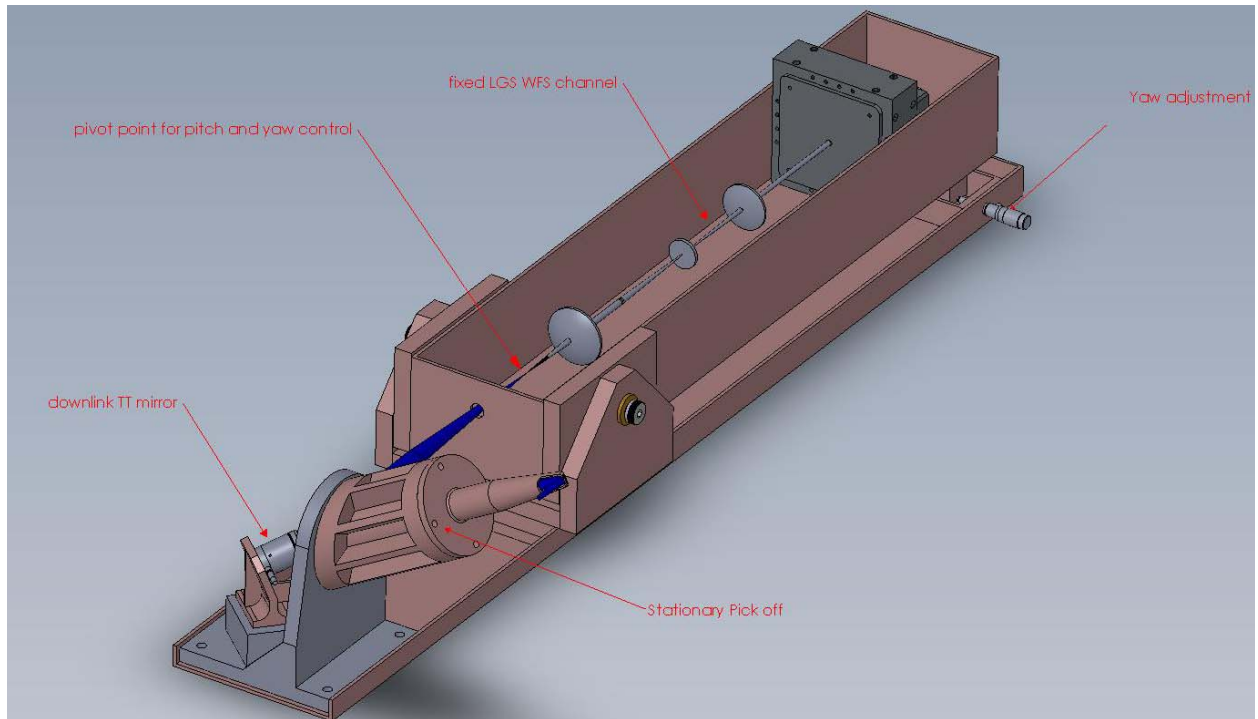
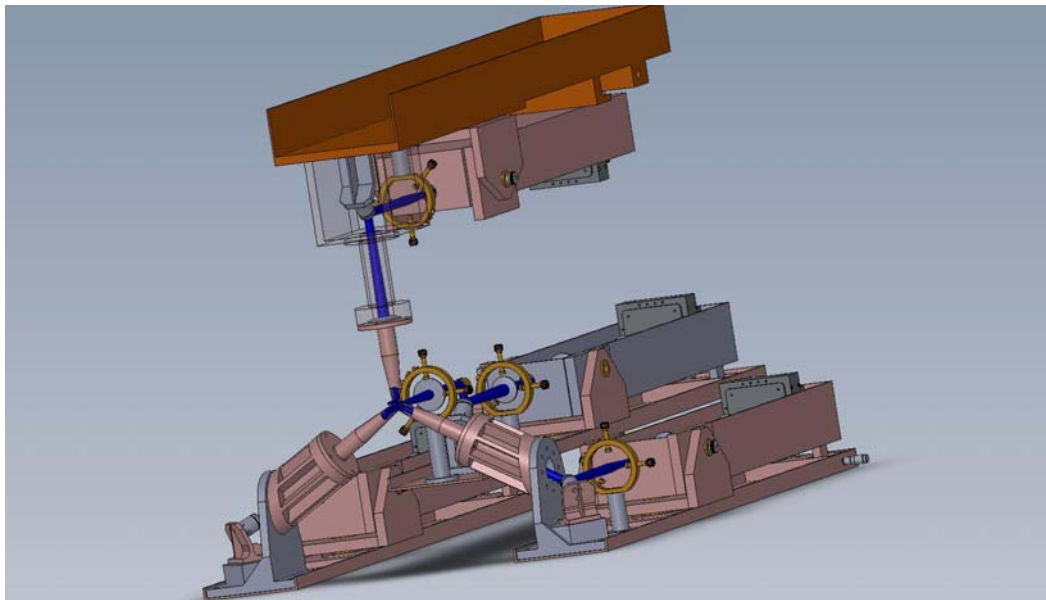


Figure 15 - Mechanical design of stationary Fixed LGS WFS channel showing the stationary 1:1 pick-off relay with the downlink tip-tilt mirror at the relay's pupil location. Each Fixed LGS WFS is equipped with yaw and pitch motion, which along with the downlink TT mirror can be used to align each channel to the incoming beam and keep the lenslet to LODM registration. [Note: Version 0.8 figure is not the latest design – will update shortly (due to travel)]



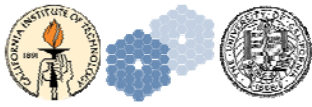


Figure 16 – Mechanical assembly of the fixed asterism pick offs and sensors assembly showing the 4 fixed LGSWFS's with one located in the middle and other three located equidistant from each other on a 10 arcsec circle about the central axis. [Note: Version 0.8 figure is not the latest design – will update shortly (due to travel)]

5.2.1.3 Fixed Asterism Shack-Hartmann WFS without Dot Relay

The LGS WFS with fewest surfaces can be made with a best shape factor singlet collimator and a lenslet array directly imaging spots onto a detector without using a reimaging relay. Sensors directly bonding a lenslet array to the face of a CCD package have been previously proven³ by University of Arizona to meet tight tolerances and have appeared to be robust if care is taken to athermalize the lenslet / CCD interface. Such a WFS is compact and has excellent optical transmission, containing only 4 transmissive surfaces. In such an approach, either the collimator or the lenslet can serve as the detector window.

For the baseline NGAO LGS WFS CCD's, having 21 um pixel pitch, such a design would require a lenslet pitch of 84 um, a lenslet focal length of 2.97 mm, and a collimator with EFL of 71.76 mm. Velur has designed such a sensor using a custom collimator and a custom lenslet, available at:

http://www.oir.caltech.edu/twiki_oir/pub/Keck/NGAO/WFS/fixed_lgs_wfs_norelay.ZMX.

Figure 17 and Figure 18 show the layout and spot diagram from this design.

The drawbacks of this approach are, potentially, the requirement for tight manufacturing tolerances for both the lenslet array and detector, elevated risk to the CCD due to additional exposed handling (and possible modification of existing packaging), and unknown long-term alignment stability and thermal-cycling behavior.

We believe it may well be worthwhile prototyping the fixturing and assembly process for such a design within the NGAO team early in the detailed design phase. However, until the identified risks are mitigated via prototyping, we have chosen to continue the PD phase design assuming the existence of a traditional “dot” relay that reforms the regular array of lenslet foci onto the CCD subapertures.

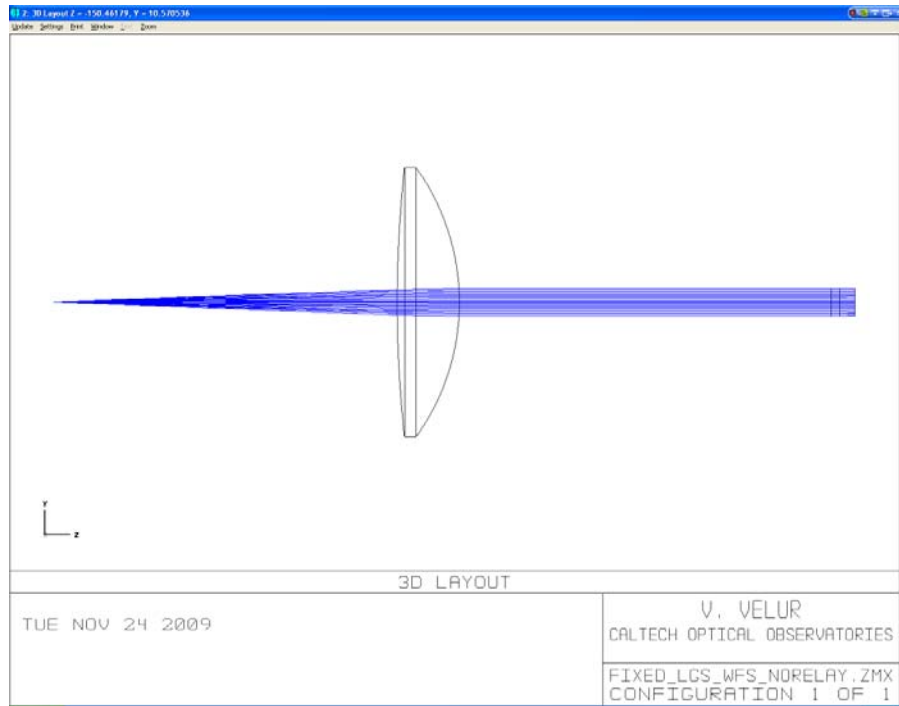


Figure 17 - Layout of the simplest possible Fixed LGS WFS wherein the lenslet spots directly imaged onto the detector (a.k.a. design without a post-lenslet relay)

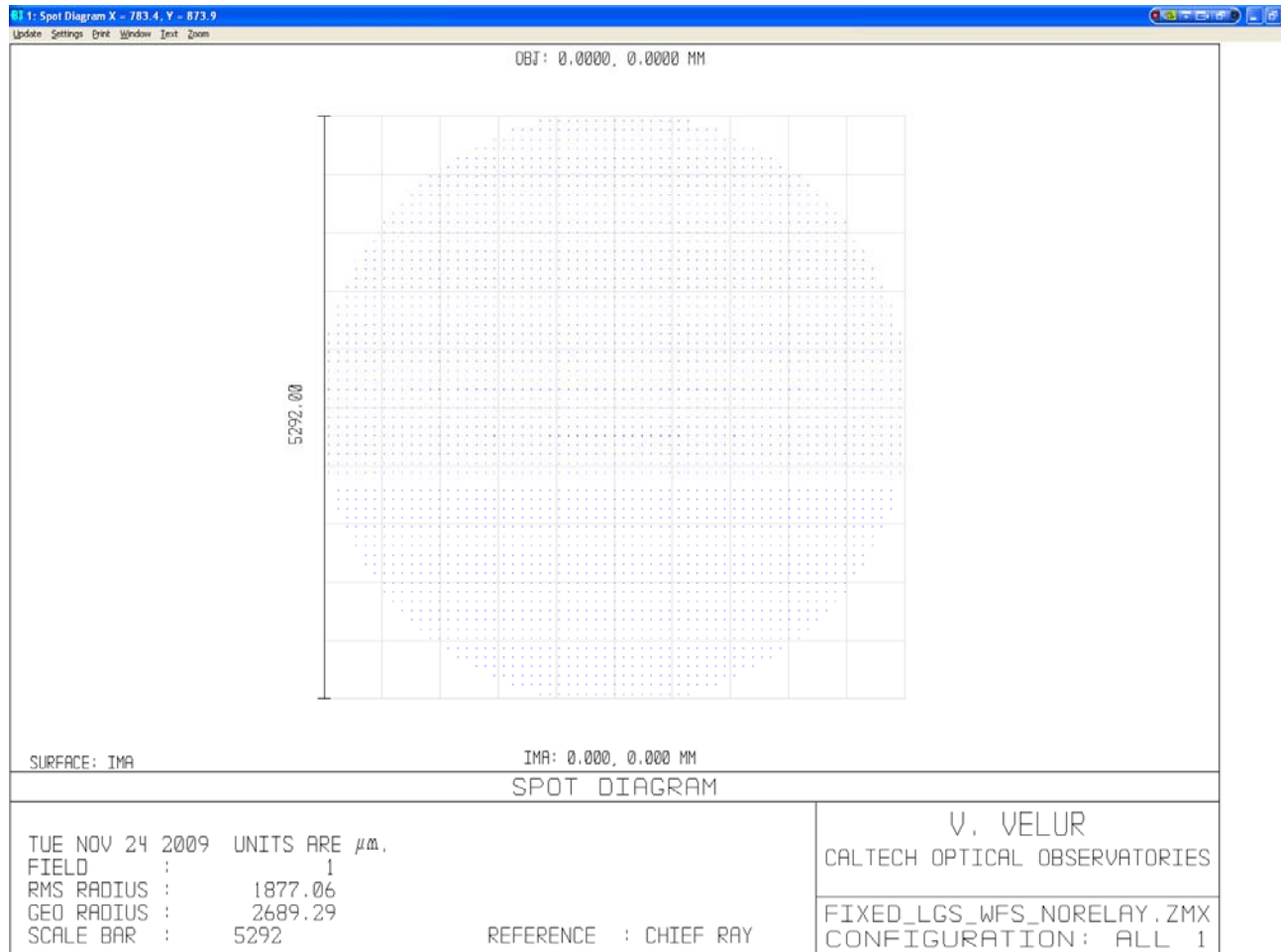


Figure 18 - Fixed LGS WFS spot diagram showing 63x63 sub-apertures from the simplest possible WFS.

5.2.1.4 Fixed Asterism Shack-Hartmann WFS with Dot Relay

The Fixed LGS WFS channels use a stock collimator, a custom lenslet and a set of two custom relay lenses. All optical components are singlets, giving rise to a total of 10 surfaces that need to be laser line coated at 589 nm. The transmission of this module is $(99.6\%)^{10} * 92.5\%$ (lenslet scatter losses) = 88.86%. The transmission of the system with the pick off (2 folds + 2 lenses) is $(99.6\%)^{16} * 92.5\% = 86.75\%$. The layout and the spot diagram from the WFS channel are shown in Figure 19 and Figure 20. The footprint diagram shown in Figure 21 indicates that the plate scale is accurate.

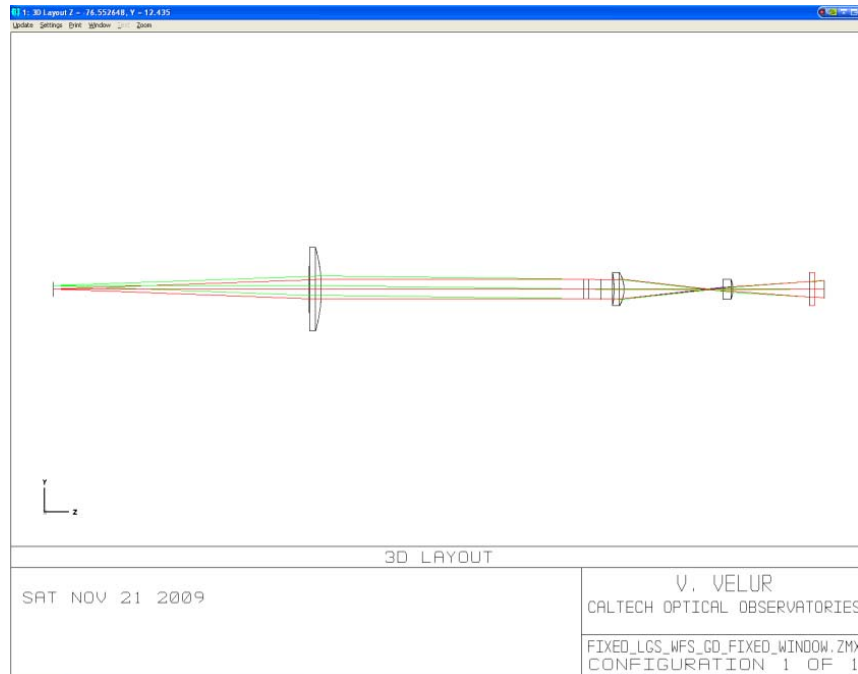


Figure 19 - Layout of Fixed LGS WFS, The total length of the sensor is 230 mm. The relay is composed of a best-form lens for a collimator, a custom lenslet array and a set of custom singlet relay lenses.

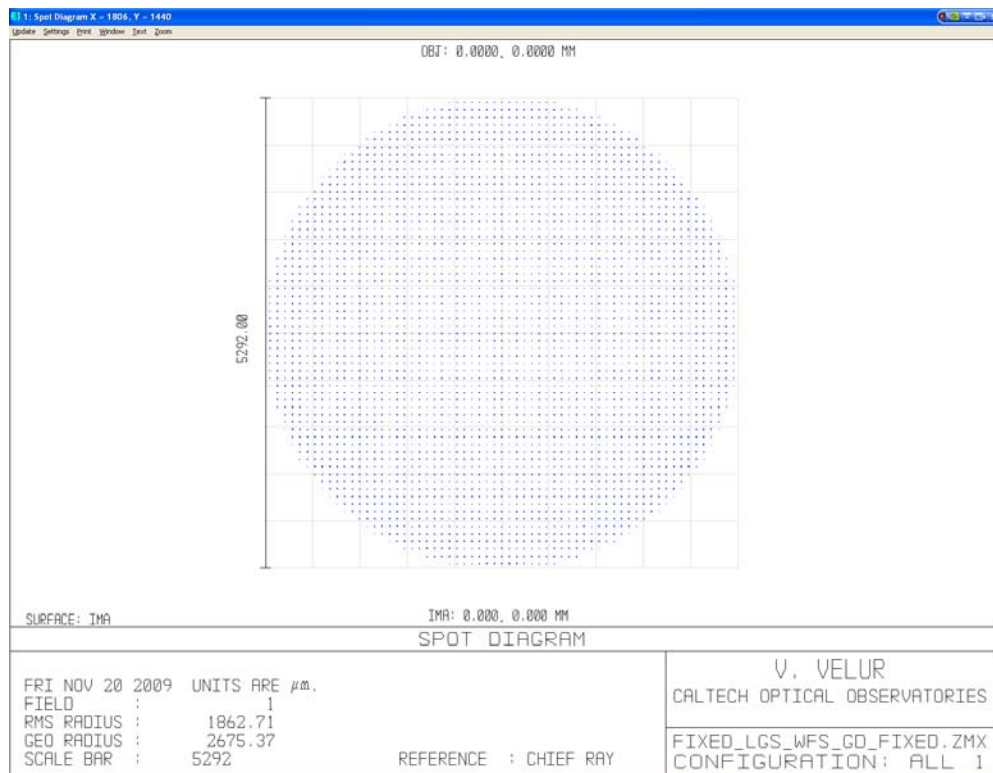


Figure 20 – Fixed LGS WFS spot diagram showing 64x64 sub-apertures

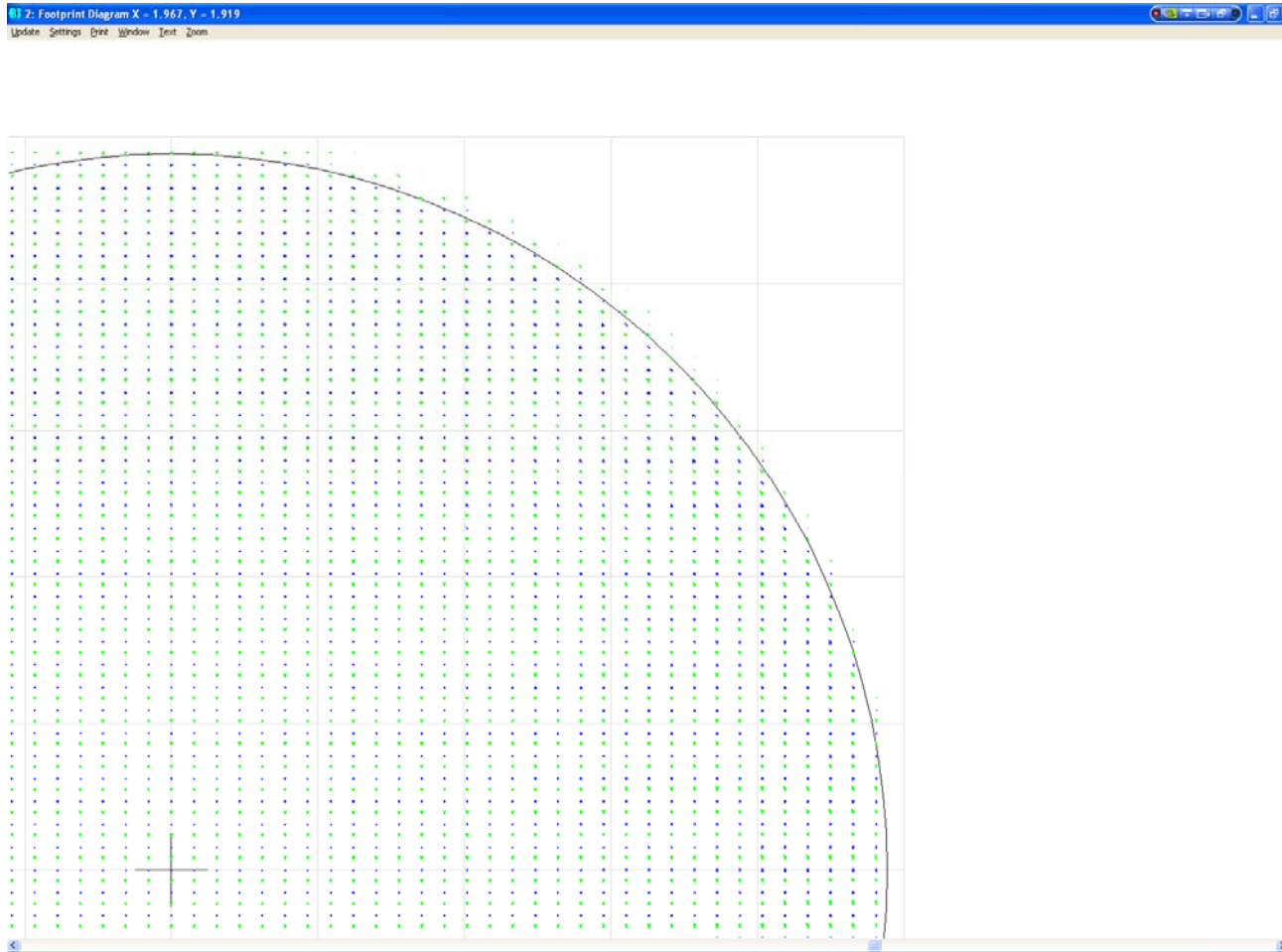


Figure 21 - Footprint diagram for a Fixed Asterism Shack-Hartmann WFS without Dot Relay, showing two field points per subaperture, one on-axis and one 1.41 arcsec (1205.7 μm) away. The separation of these points confirms the plate scale at the detector is 0.705arcsec/pixel.

5.2.1.5 Fixed LGS WFS Post-lenslet Relay

To ensure that the requirement on the wavefront quality delivered by the WFS relay, the relay was modeled separately and the image quality of the relay assessed independently. The layout of the relay is shown in Figure 22. The relay delivers sub 1 μm RMS spots with a 0.03% grid distortion at a de-magnification of 0.89.

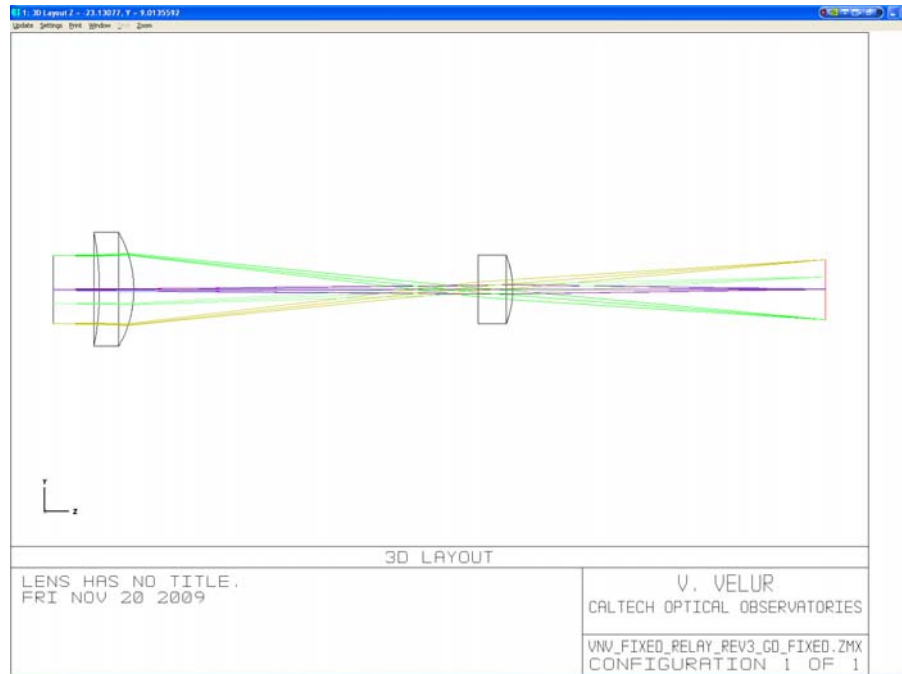


Figure 22 - Fixed LGS WFS post-lenslet WFS relay layout.

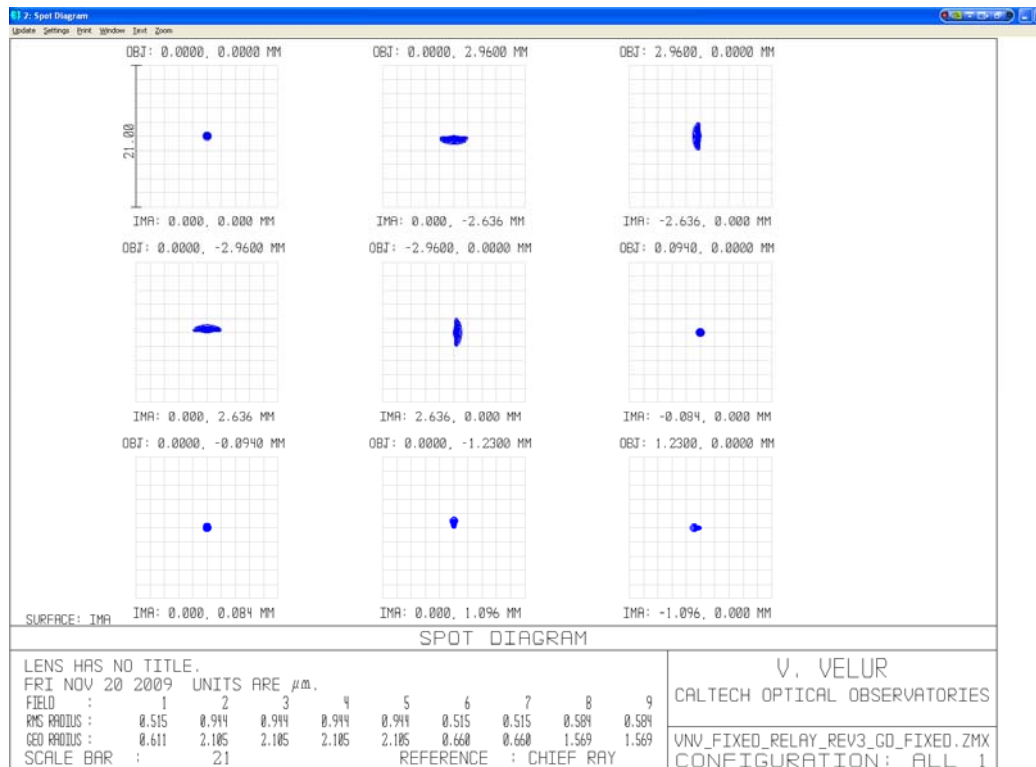


Figure 23 – Spot diagram showing an on-axis point and 4 extreme points of the lenslet spots with the worst case spot size being 0.95 μm RMS radius. Detector pixel size is 21 μm for reference. Field



points 6 and 7 are one lenslet spot away indicating that the magnification is matched to 84 um spot separations at the detector. The grid distortion of the relay is 0.03%.

5.2.2 Patrolling LGS WFS

5.2.2.1 Patrolling Asterism WFS Design Parameters

As indicated earlier, the p-value (e.g. the ratio of pixel size to spot size) for the Fixed LGS WFS is 1.0. Hence, 1.49 arcsecs on-sky corresponds to one detector pixel (21 um). From the NGAO optical design, we know that 720 um at the LGS focal plane corresponds to 1 arcsec on-sky. The Patrolling WFS pick-off is a 1:2 relay making the plate scale at the focus to the WFS 1440 um/arcsec.

Also, Plate Scale Ratio (PSR) = $f_{\text{collimator}}/f_{\text{lenslet}} * 1/m$ = Plate scale at the input of the sensor (um/asec)/ Detector plate scale (um/asec) = $720*2/14.0939 = 102.171$, where m is the de-magnification between the lenslet spots and the detector.

The pitch of the lenslet array is given by, $d_{\text{each lenslet}} = (f_{\text{collimator}}/f\#) * 1/(\# \text{ of sub-aps}) = 95/27.12 * (1/31) = 113 \text{ um}$.

The de-magnification, $m = (\text{spot separation at detector} / \text{lenslet pitch}) = (0.021*4)/0.113 = 0.74$, we choose, $f_{\text{collimator}} = 95 \text{ mm EFL}$ from JML Optical's catalog.

The focal-length of the lenslet is, $f_{\text{lenslet}} = f_{\text{collimator}}/m * (\text{PSR}) = 95/0.74337 * (1/102.1714) = 1.25 \text{ mm}$. The F/# of the lenslet is = 11.06.

The Fresnel Number (FN#) of the lenslet, $\text{FN\#}_{\text{lenslet}} = (d_{\text{each lenslet}}/2)^2/(f*\lambda) = 4.33$.

5.2.2.2 Patrolling Asterism Pick-off Relay

A 1:2 telecentric relay was designed to accommodate mechanical packaging of the theta-phi pick-off and the fast TT mirror located at the relay pupil. The total length of the relay is 528 mm. Figure 25, Figure 26, Figure 27 show the spots from the relay and the mechanical assembly of the pick-off arm and the 3 channel Patrolling WFS assembly. The pick off mirror location is +10, -5 and -20 mm from the focal plane for the 3 Patrolling WFS. The light that is incident on the pick-off gets folded and collimated to form a pupil at fast TT mirror which folds the beam down to a pair of periscope mirrors. The pick-off mirror and the fast TT mirror are part of the rotatable lever and the periscope mirrors are part of a rotating crank. The combination of these two rotations facilitates positioning the pick-off anywhere in the field. The design of the pick-off relay can be downloaded from

http://www.oir.caltech.edu/twiki_oir/pub/Keck/NGAO/WFS/pns_pick_off.ZMX.

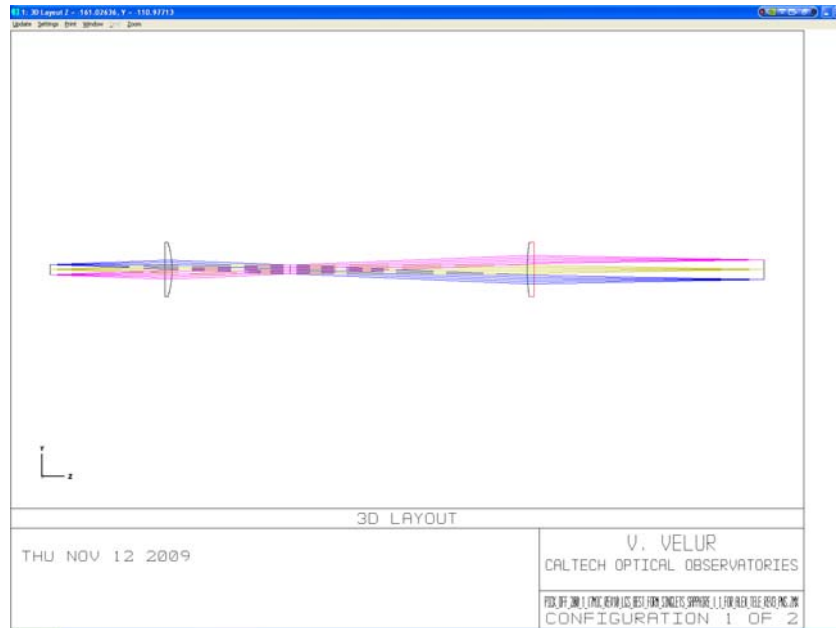


Figure 24 – Figure showing the telecentric unfolded layout of the Patrolling LGS WFS pick off. The relay is 1:2 due to packaging constraints (having to get these WFS out of the way of the interior Fixed Asterism WFS's).

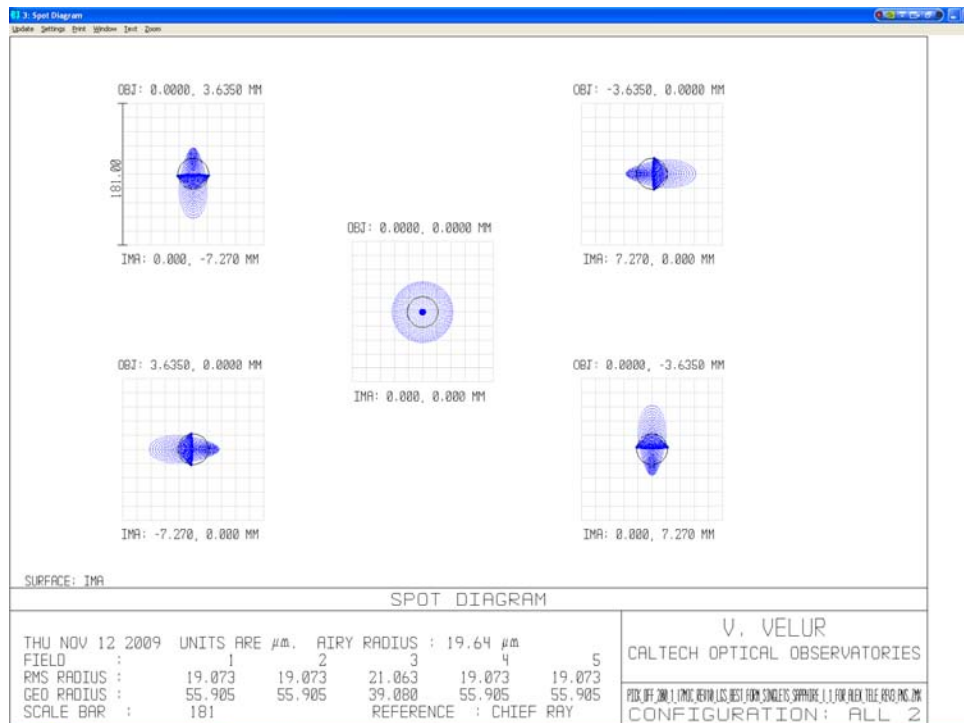


Figure 25 – Spot diagrams from the 1:2 Patrolling WFS pick-off relay showing spots with rms spot radius of 21 μm as compared to 130 μm rms spots delivered by the AO relay. For reference 181 μm is 1/4 arcsec.

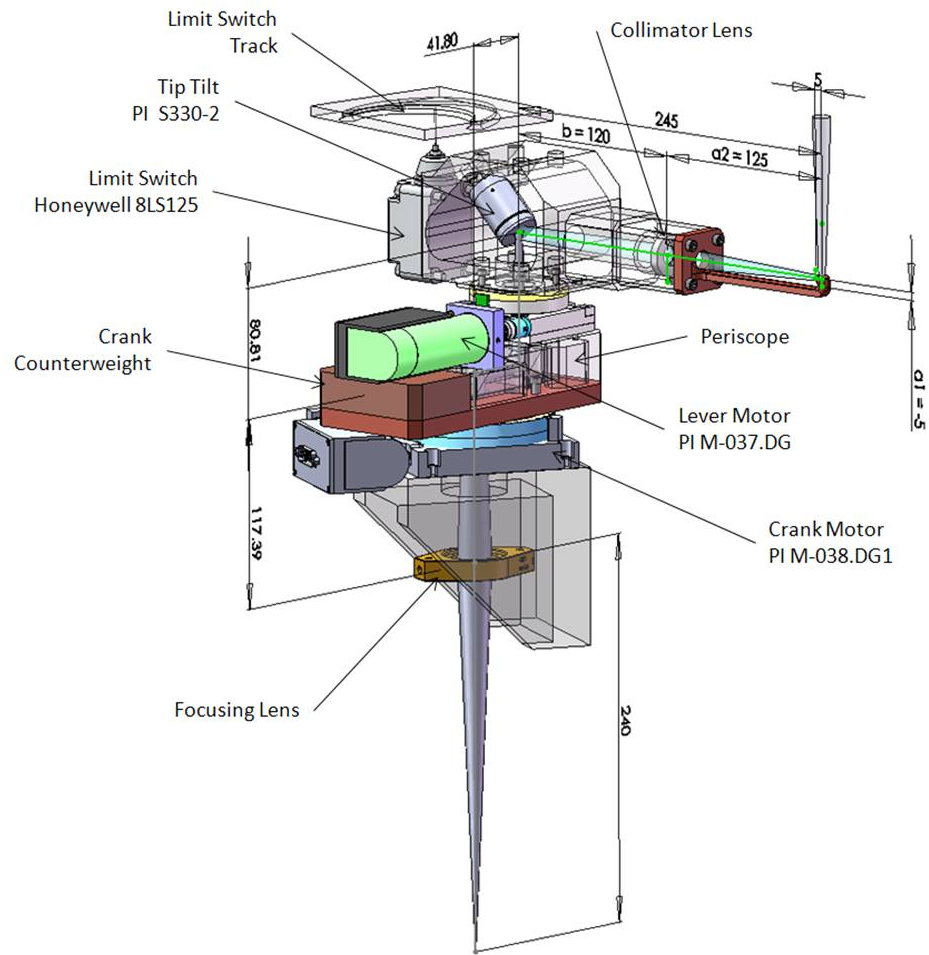


Figure 26 - Mechanical assembly of a single Patrolling WFS pick-off OSM showing the theta-phi mechanism with a downlink TT mirror located at the pupil.

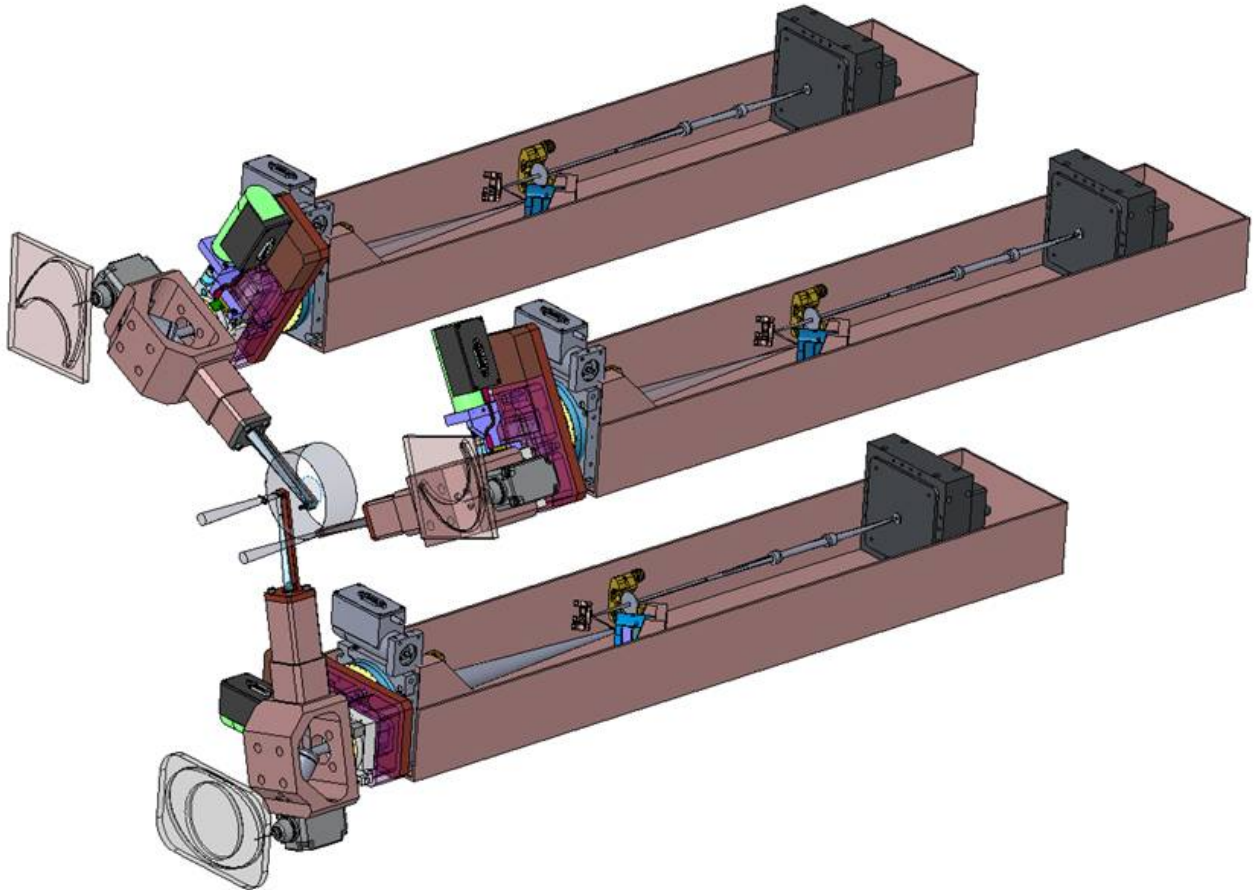


Figure 27 – Mechanical assembly of the Patrolling WFS channels showing the lenslet, the post-lenslet relay and the WFS CCD camera. Each of the Patrolling WFS channel is also equipped with a TT mirror near the focus of the pick-off relay to keep the DM pupil registered onto the lenslet; this is necessary to eliminate pupil wander as each OSM patrols the entire 120" LGS FoR.

5.2.2.3 Patrolling Asterism Shack-Hartmann WFS without Dot Relay

A relay-less Shack-Hartmann WFS for the Patrolling Asterism would differ from the corresponding Fixed Asterism WFS only slightly, in order to optimize for the particular image FWHM expected in the Patrolling WFS. Such a WFS would have a lenslet pitch of 84 μm and lenslet focal length of 0.69 mm with a 70.62 mm EFL collimator. For completeness, such a sensor was designed by Velur and the design is available at: http://www.oir.caltech.edu/twiki_oir/pub/Keck/NGAO/WFS/PnS_lgs_wfs_norelay.ZMX.

Figure 28 and Figure 29 show the layout of this sensor and the spot diagram at the detector plane.

For reasons described in Section 5.2.1.2, until risk can be mitigated for this approach, we will continue in the PD phase assuming a traditional design utilizing a post-lenslet array optical “dot” relay.

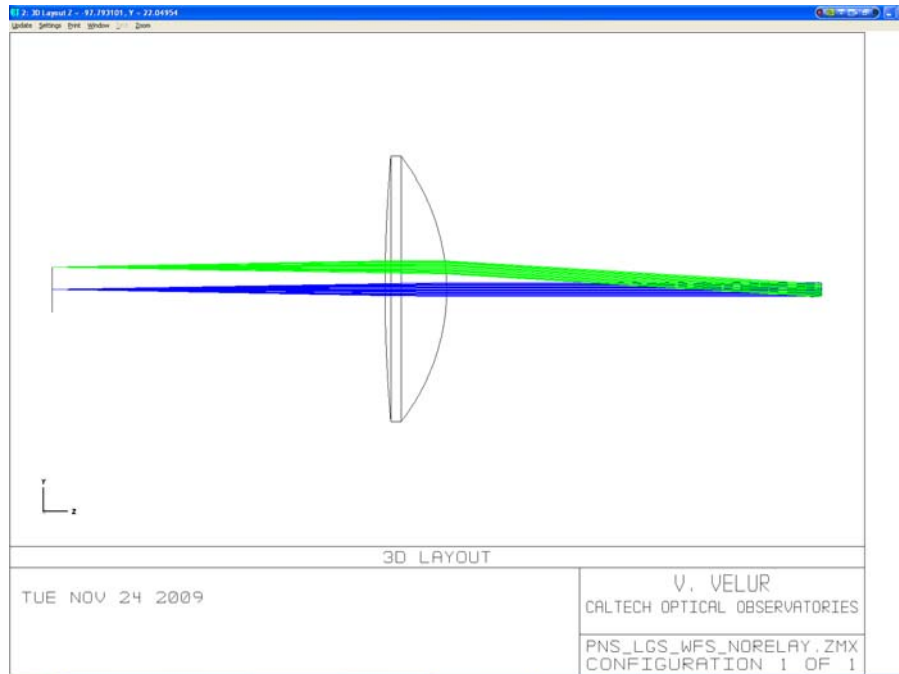


Figure 28 - Layout of the simplest possible Patrolling LGS WFS wherein the lenslet spots directly imaged onto the detector (i.e. design without a post-lenslet relay)

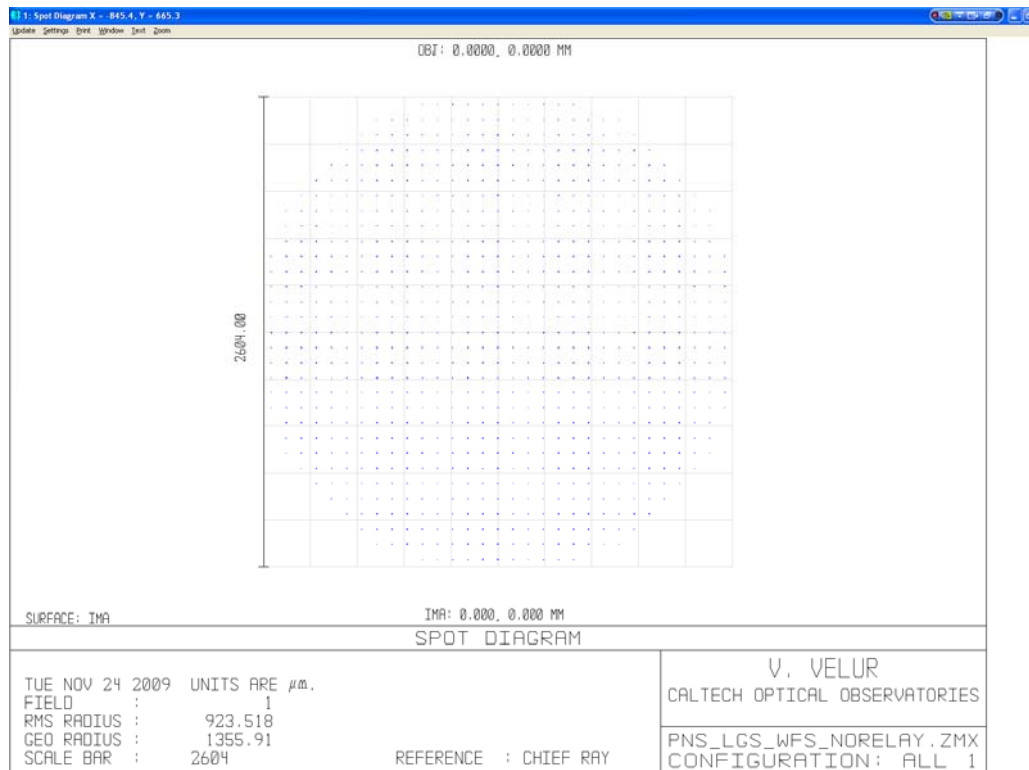


Figure 29 - Patrolling LGS WFS spot diagram showing 31x31 sub-apertures from the simplest possible WFS design.



5.2.2.4 Patrolling Asterism Shack-Hartmann WFS with Dot Relay

The Patrolling WFS also uses a commercial best-form collimator lens followed by a custom lenslet and relay lenses. The design of the WFS can be obtained from: http://www.oir.caltech.edu/twiki_oir/pub/Keck/NGAO/WFS/PnS_lgs_wfs_doublets_rev1_window.ZMX. The WFS spots are shown in Figure 31 and a footprint diagram was used to verify the plate scale of the sensor. The total length of the sensor is 490 mm.

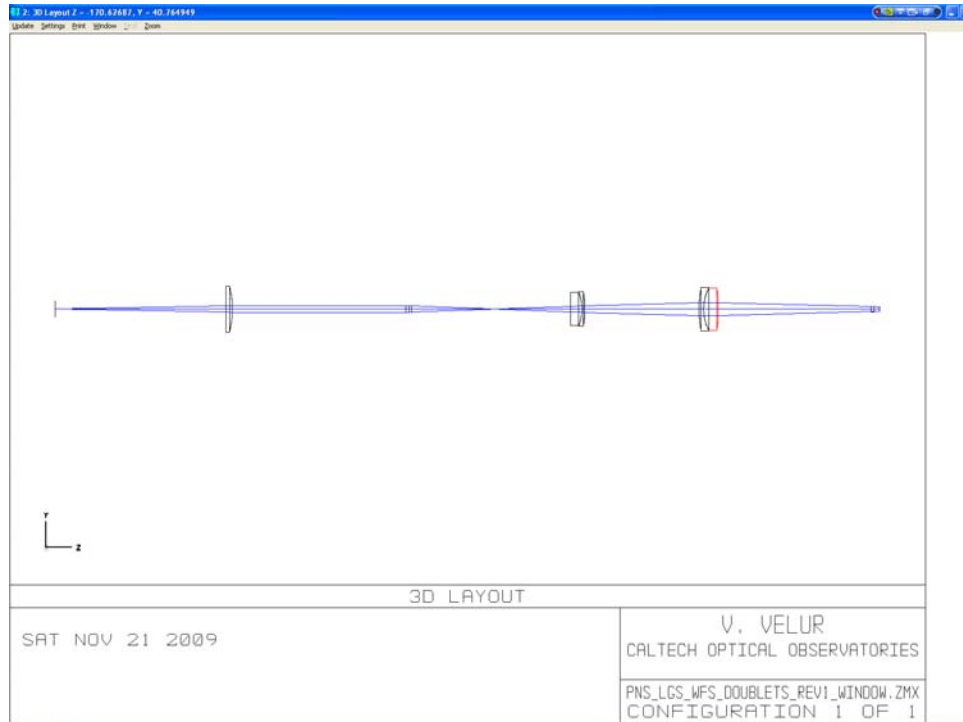


Figure 30- Layout of the Patrolling WFS; the total length of the sensor is 490 mm. [Note: I can make the relay longer to get better spots at the detector).]

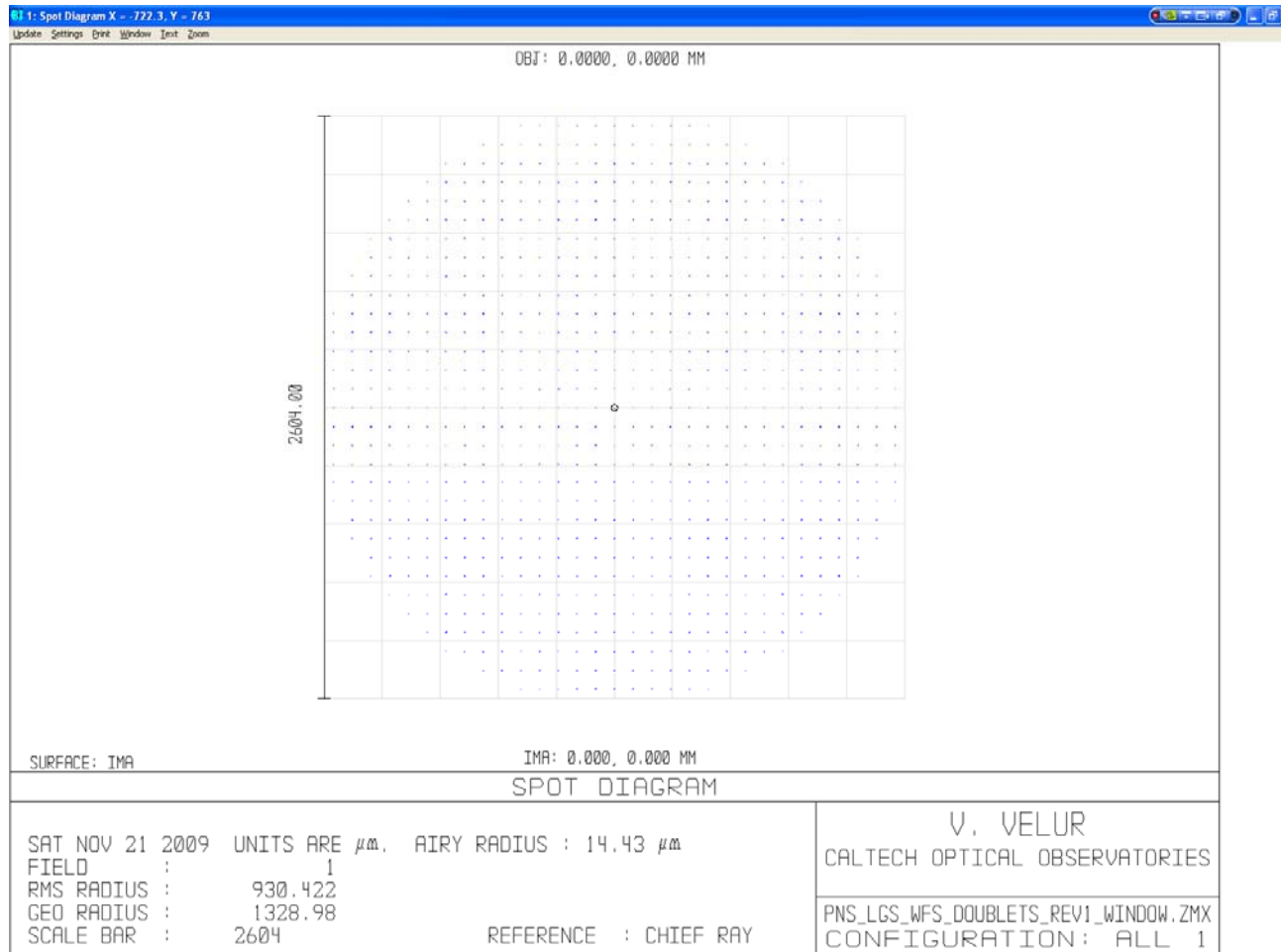


Figure 31 - Spot diagram at the detector

5.2.2.5 Patrolling LGS WFS Post-lenslet Relay

The post lenslet relay was modeled separately for the Patrolling WFS and the performance of the relay measured. Since the lenslet spots are f/11 the design required doublets rather than just a pair of singlets. Models were built with single doublet and a singlet field lens with unsatisfactory performance. The 2 doublet relay gives sub um (RMS) spots with negligible grid distortion.

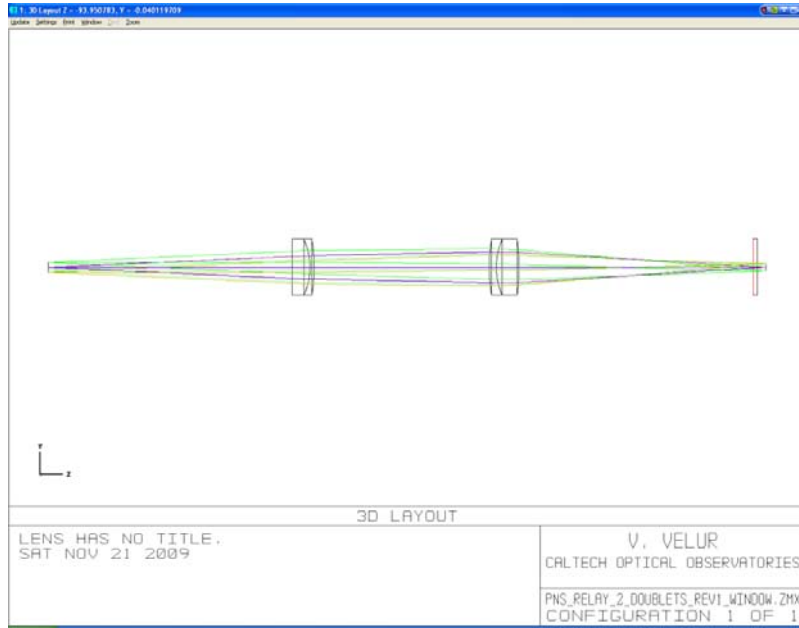


Figure 32 – Shows the layout of the post lenslet relay in the Patrolling LGS WFS. The length of the relay is 300 mm.

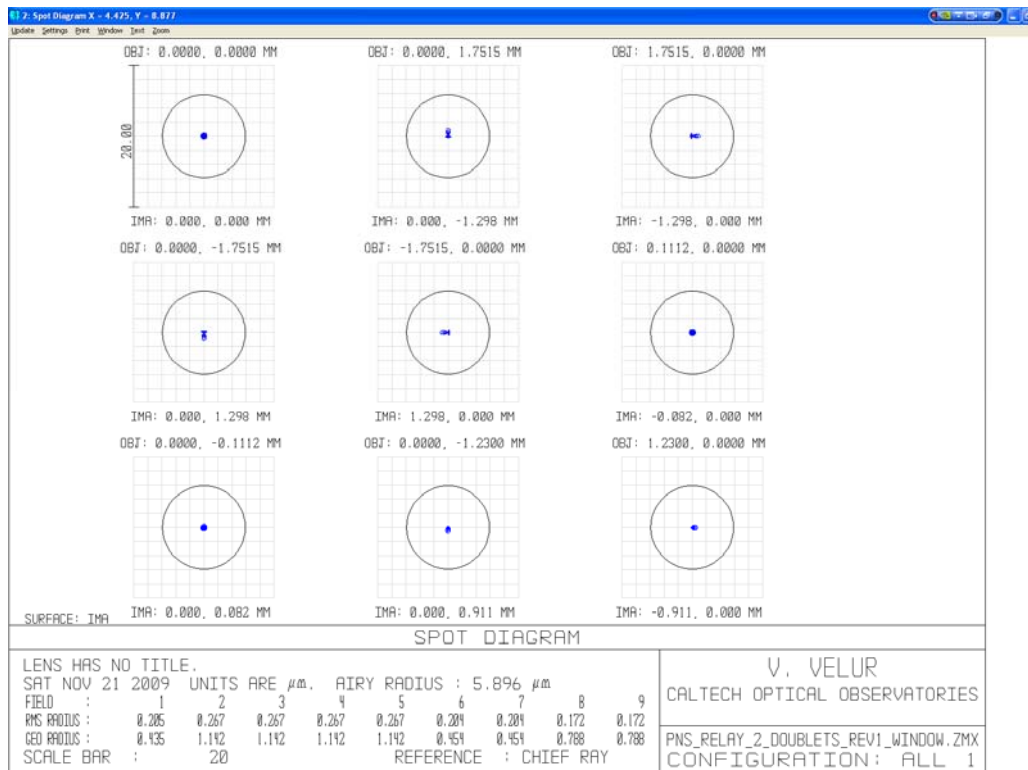


Figure 33 - Spot diagrams of the relay with on-axis and extreme field points (field #s 2 through 5). There are also 2 field points to indicate that the magnification (field #s 6 and 7) is correct and 2 more located at $1/\sqrt{2}$ of the field size. The grid distortion of the relay is 0.001%.



5.2.3 Performance of the LGS WFS including the AO relay

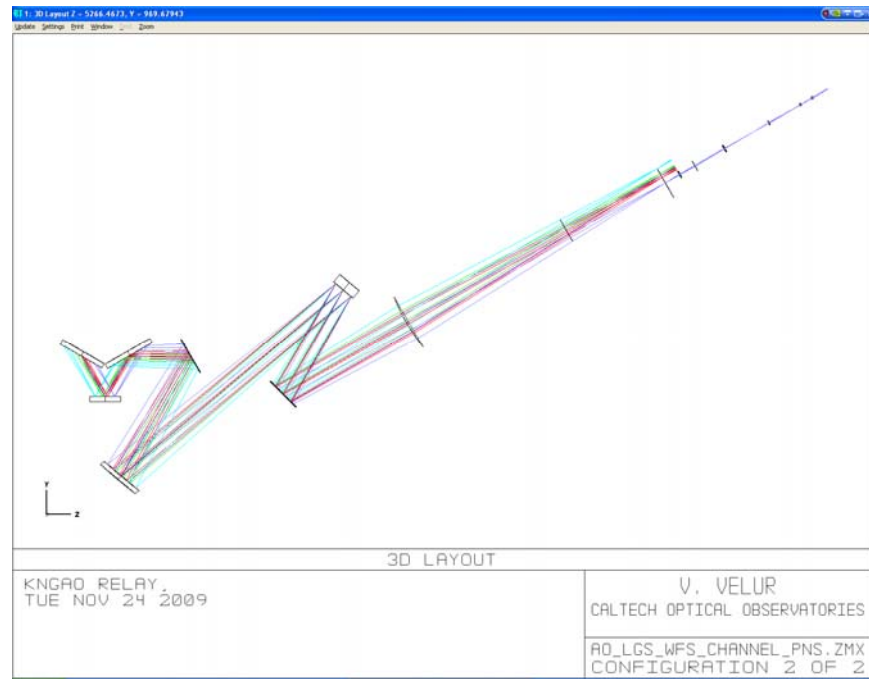


Figure 34 - NGAO optical path for Fixed Asterism LGS WFS [Note: this figure will be updated with a correctly folded LGS WFS channel].

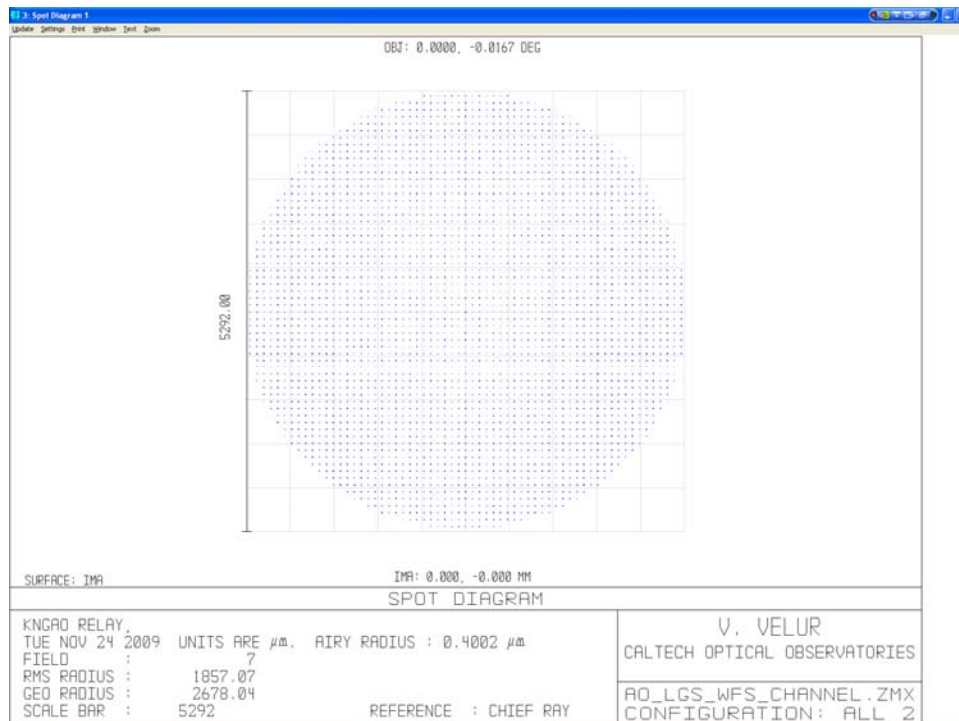


Figure 35 - Footprint diagram for full optical path of Patrolling Asterism LGS WFS

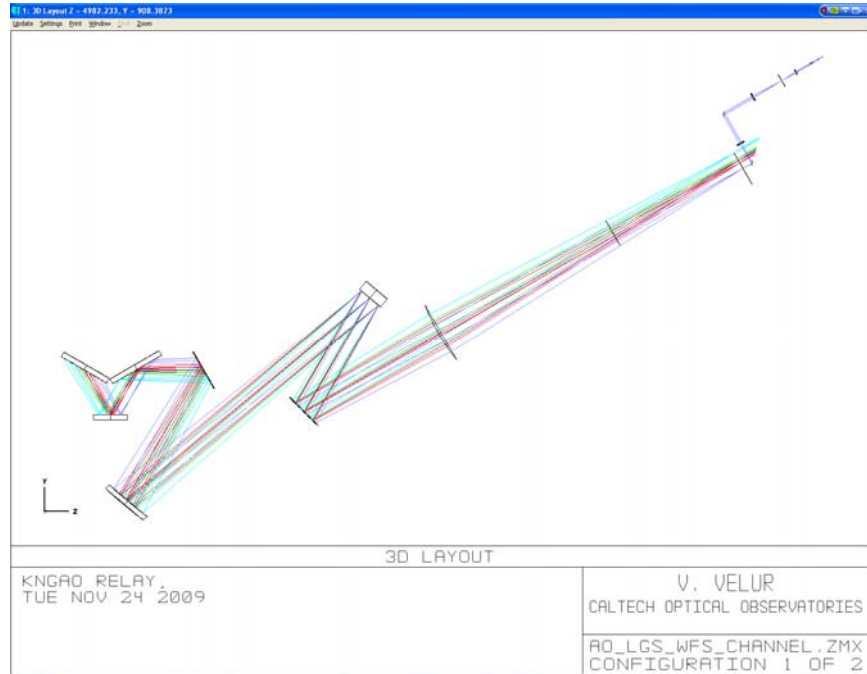


Figure 36 - NGAO optical path for Patrolling Asterism LGS WFS [Note: this figure will be updated with a correctly folded LGS WFS channel].

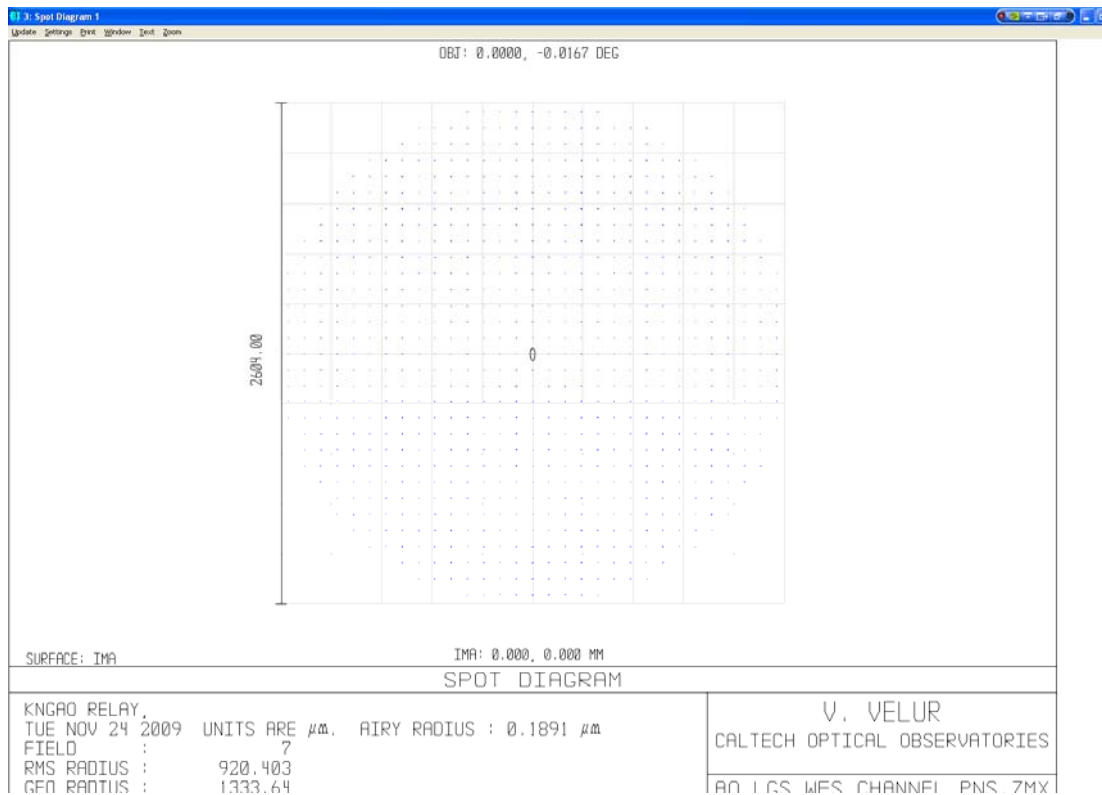


Figure 37 - Footprint diagram for full optical path of Patrolling Asterism LGS WFS.



Blurring of Shack-Hartmann spot		
Error source	Tomo. LGS WFS spot size	PnS LGS WFS spot size
AO relay	20 mas	20 mas
Focal plane curvature	0	
OSM	50 mas	50 mas
WFS relay	60 mas	60 mas
Allocation	250 mas	250 mas
Diffraction spot size (for ref.)	785 mas	290 mas

Shift of the worst case sub-ap. from the crosshair		
Error source	Tomo. LGS WFS spot size	PnS LGS WFS spot size
AO relay	20 mas	120 mas
Focal plane curvature	22 mas	
OSM	TBD (based on ray fan)	TBD
WFS relay	TBD	TBD
Allocation (10% of sub-ap.)	300 mas	600 mas
Diffraction spot size (for ref.)	785 mas	290 mas

Distortion		
Error source	Tomo. LGS WFS spot size	PnS LGS WFS spot size
AO relay		
Focal plane curvature		
OSM		
WFS relay		
Allocation (10% of sub-ap.)		
Diffraction spot size (for ref.)		

Table 5 Overall design errors showing the LGSWFS design meeting allocations

	Fixed LGSWFS	Patrolling LGSWFS
P value	0.5	1
Plate scale	.705"/pixel	1.49 "/pixel
Capture range	1.5*2 waves	2.5*2 waves
lambda/d	710 mas	355 mas
Capture range	2.13 arcsec	1.775 arcsec
1d tilt (RMS)	50 mas	100 mas

Table 6



5.3 Mechanical Design

The mechanical packaging of the seven wavefront sensor channels of the NGAO LGS WFS is made challenging by the tight packaging requirements for the selection of multiple LGS with a relatively small (< 90 mm) diameter wide-field relay output focal plane. To create space between different LGS channels, we have adopted a design based fundamentally upon the ‘fisherman-around-the-pond’ approach previously explored for deployable-IFU spectrographs and explored in the design of the four-Shack-Hartmann-channel Palomar multiple guide star wavefront sensor. The overall mechanical package for the LGS WFS is shown in Figure 38 and Figure 39.

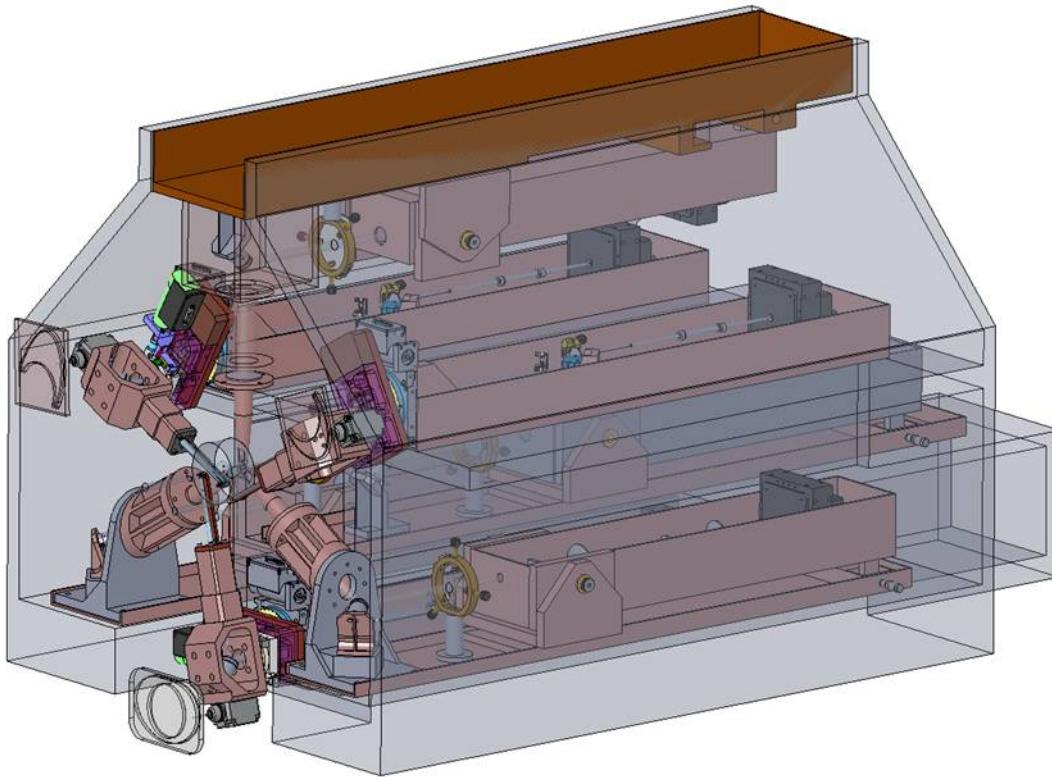


Figure 38 – Full mechanical assembly of the LGS WFS within a notional housing (support structure not shown)

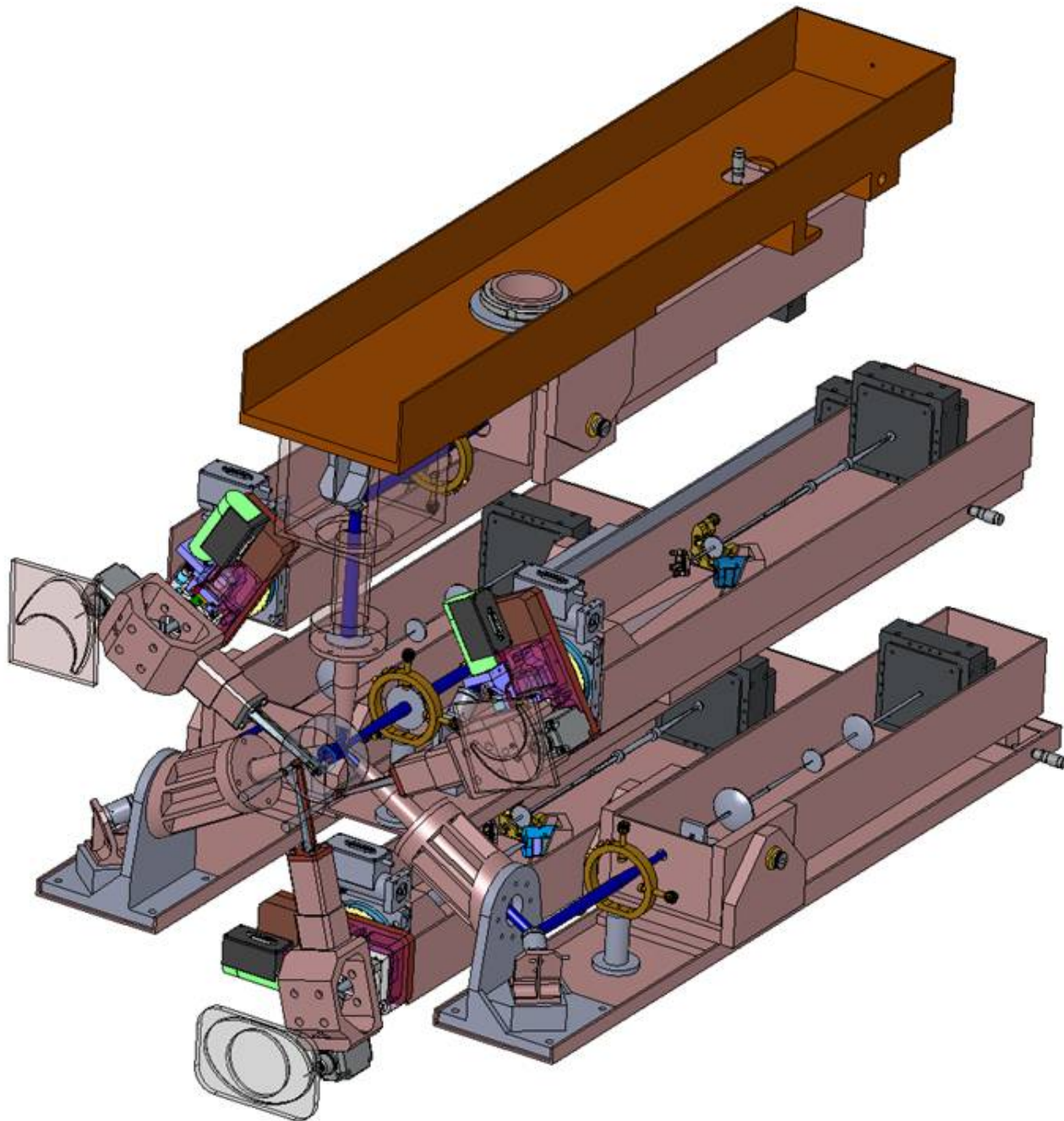


Figure 39 - Full mechanical assembly of the LGS WFS with housing removed.

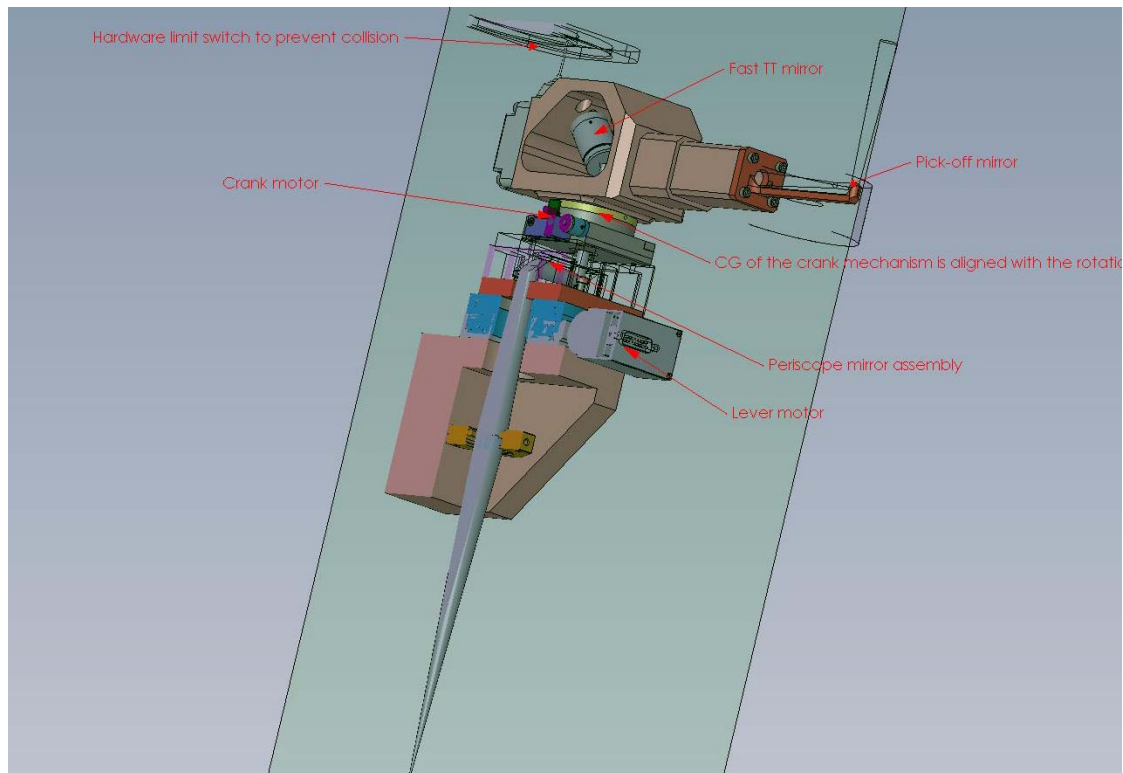


Figure 40 - Part cross sectional view of the Patrolling LGS OSM pick-off

5.3.1 WFS Pick-off and WFS Relay

Figure 40 shows a partial cross-sectional view of the Patrolling WFS pick-off. The theta-phi pick off is better than the r-theta as it doesn't need refocusing (and there the pupil mapping geometry is maintained at all field positions). The crank arm and the lever arms are balanced about their axis of rotation and to prevent torque on the motor at any position of the arm. A Honeywell 8LS125 micro-switch and a custom contour milled track serve the purpose of a fail-safe system to prevent collision of the pick-off arms with its surrounding in case of software failure. The crank and lever motors use PI's M037 and M-038 drives. M-037 rotation stages are equipped with ultra-precise worm gear drives allowing unlimited rotation in either direction. Model M-037.DG is a closed-loop DC motor with shaft-mounted position encoders and precision gearheads providing $3.5 \mu\text{rad}$ at a design resolution of $0.6 \mu\text{rad}$. Model M-038.DG1 is equipped with a closed-loop DC motor with shaft-mounted position encoder and precision gearhead providing minimum incremental motion of $3.5 \mu\text{rad}$ at a design resolution of $0.6 \mu\text{rad}$. A frictionless high-precision flexure based PI's S-330.8SL TT stage with an invar platform houses the TT mirror. This stage has excellent temperature stability and works all the way to -20 degrees C. Calculations in Section 5.1.2 show that this mirror amply serves its purpose. The specifications for the TT mirror can be found at:



<http://www.physikinstrumente.com/en/products/prspecs.php?sortnr=702900>. There is a pair of periscope mirrors mounted on the crank motor and there is a focusing lens past the second periscope fold mirror. Appropriate jigs will be designed to mount the mirrors at the exact angle onto each surface on which it is to be held.

The fixed asterism uses a simpler stationary pick-off. A snout-like part holds the pick-off mirror which folds the light into a barrel with a collimator followed by a TT mirror (also a PI S-330.8SL). The specs for the TT mirror can be found at <http://www.physikinstrumente.com/en/products/prspecs.php?sortnr=300700>. There is a focusing lens following the TT mirror that feed light to the WFS optics. U-channels are used to house all 7 WFS optics and detector to keeping the deflection to below $1/10^{\text{th}}$ of the finest sub-aperture.

5.3.2 Baffles, Enclosure and Linear Focus Stage

Each WFS will be baffled to reduce effects of Rayleigh backscatter effects by enclosing the whole WFS relay except for the field-stop. An enclosure made of sheet metal over the aluminum structure will be used to keep the LGS WFS clean. The whole WFS assembly shall be mounted on a 205 mm (focus required to track the sodium layer between 80 and 292 km distance from the telescope) travel linear stage. An Aerotech ABL20030 stage with 300 mm travel will be used to move the whole assembly to track the change in distance to the Na-layer. The specs for the stage can be found at <http://www.aerotech.com/products/airbearing/abl2000specs.html>. The stage is a fully-preloaded air-bearing stage with a brushless linear motor. The package is zero-maintenance.

5.3.3 Pupil Registration and TT Corrector

Because the LGS light path to the WFS is not perfectly telecentric it is necessary to register the DM actuators and the lenslet for each point in the field for the Patrolling WFS (if the effect is not measured and calibrated). For this process we have a slow TT mirror near the pick-off focus to register the LODM actuators to the lenslet. We also provide a pitch and yaw mechanism to align the fixed LGS WFS lenslets to the LODM. Each LGS arm has a downlink TT mirror, located at the pupil formed in the pick-off mechanism, to correct the differential motion LGS light with respect to the desired centroid location.

5.4 Tolerancing

5.5 Requirements Compliance

The requirements compliance matrix can be found at:

http://www.oir.caltech.edu/twiki_oir/pub/Keck/NGAO/091207_LGS_WFS/1.2.7-LGS_WFS_Functional_Requirements_091121_v2.pdf



5.6 Risk Register and Risk Mitigation Plan

A risk register and mitigation plan can be obtained from:

http://www.oir.caltech.edu/twiki_oir/pub/Keck/NGAO/091207_LGS_WFS/091207_LGS_WFS_PD_Risk_Register_v1.pdf

5.7 Work left to do

The following list of outstanding issues is expected to be addressed in full prior to the Preliminary Design Review:

Stray light (including Rayleigh scatter) analysis

Simplification of the Optical Design of sensors if possible.

Try to redesign the plano-(parabolic) convex lens to try and provide less aberrated LGS spots at the LGS assembly input.

Cost reduction by finding more economical components for motion control.

Draft interface documents between the LGSWFS assembly and the various other sub-systems.

Detailed cost estimate revision, in support of the PD Phase NGAO Cost Book.

¹ Comparison of centroid computation algorithms in a Shack–Hartmann sensor, S. Thomas et. al, MNRAS 2006

² Study of optimal wavefront sensing with elongated laser guide stars, S.J.Thomas et. al., MNRAS 2007

³ McGuire, P. C., et al., “[Construction and testing of the wavefront sensor camera for the new MMT adaptive optics system](#)”, *Proc. SPIE* TBD (TBD).